

Applied and
Computational
Mathematics
Division

NISTIR 89-4121

Center for Computing and Applied Mathematics

*A Mechanism for Shear Band Formation
in the High Strain Rate Torsion Test*

Timothy J. Burns

June 1989

U.S. DEPARTMENT OF COMMERCE
National Institute of Standards and Technology
Gaithersburg, MD 20899

QC
100
U56
89-4121
1989
C.2

NISTC
QC100
.456
NO.89-4102
1989
C.2

Abstract

An asymptotics argument is given, which shows that rigid unloading from the ends of the thin-walled tubular specimen, enhanced by conductive heat transfer, is a plausible mechanism for adiabatic shear band formation during the high strain rate torsion test. The argument assumes that thickness variations, as well as elastic and dynamic effects in the tube, can be ignored, but that heat conduction and heat-sink thermal boundary conditions must be included. The proposed mechanism is supported by a numerical analysis of a mathematical model of the torsion test, which is based on recent torsional Kolsky bar experimental work of Marchand and Duffy (1988), on a physical model of thermoelastic-plastic flow due to Wallace (1985), and on a phenomenological Arrhenius model of the plastic flow surface. The numerical technique used is the semi-discretization method of lines.

1. Introduction

It has been known for a long time that, during the late stages of large strain plastic deformation at high strain rate, such as occurs during penetration of armor by ballistic impact or during high-speed machining, the accumulated permanent strain can become highly localized (see, *e.g.*, the review by Rogers (1979)). Zener and Hollomon (1944) proposed that the basic mechanism for this localization is a dynamic instability caused by adiabatic heating. That is, when the deformation takes place so rapidly that there is not enough time for heat conduction to take place over an appreciable length scale, the tendency of a ductile metal to harden with increasing plastic strain is eventually counterbalanced and then dominated by a tendency to soften with the rapid temperature increase associated with the dissipation of plastic work into heat. Unfortunately, although this strain localization is believed to be driven by shear stress, a penetration event or a rapid machining process involves a large mean compressive stress as well, which makes detailed analysis of such a deformation formidable.

Thus, it is not surprising that a great deal of interest has been stimulated by the high strain rate torsional Kolsky bar experimental work of Costin, *et al.* (1979), Hartley, *et al.* (1987), and most recently, Marchand and Duffy (1988), who observed the formation of a single shear band in thin-walled steel tubes under loading conditions which are essentially the same as occur in rapid simple shear (see, *e.g.*, Shrivastava, *et al.* (1982)). Successively improved measurements of the local temperature rise as the deformation localized into a single adiabatic shear band were also obtained. In addition, Marchand and Duffy (1988) recorded

the evolution in time of the inhomogeneous strain distribution. This was done by photographing an originally horizontal grid pattern, which had been etched on the outer walls of the tubes parallel to their axes prior to the tests, at different times during the experiments. On the basis of the experimental results, the authors concluded that shear strain localization at high strain rate can be divided into three stages, associated with strains γ_I and γ_{II} , with $\gamma_I < \gamma_{II}$. During the first stage, for nominal plastic shear strains $\gamma < \gamma_I$, the grid lines were observed to remain straight while they tilted to an angle δ uniformly around the tubular samples, where $\gamma = \tan \delta$. During the second stage, for $\gamma_I \leq \gamma \leq \gamma_{II}$, the grid lines were observed to curve, so that the deformation had begun to localize, uniformly around the samples. For nominal shear strains satisfying $\gamma > \gamma_{II}$, the flow stress was observed to drop rapidly, the shear bands were observed to narrow considerably, down to about $20 \mu\text{m}$ in the HY-100 steel, and a strong dependence of shear strain on the circumferential coordinate around the tubes was observed.

Even under the comparatively simple loading conditions of the torsion test, there is no consensus in the literature on the details of the evolution of the inhomogeneous strain field. Although Marchand and Duffy (1988) believed that the flanges on the ends of the thin-walled tubes in their experiments provided heat sinks, and that the stress remained homogeneous throughout their tests, except at very early time and after a narrow shear band formed, they cited the papers of Litonski (1977), Wright and Walter (1987), and of Molinari and Clifton (1987) as providing numerical predictions which were qualitatively consistent with their experimental results. In Litonski (1977), and in Molinari and Clifton (1987), the assumptions were made that the mid-section of the thin-walled tube was thinner than the outer portions of the tube, and that the tube was in mechanical equilibrium during the test, so that the shear stress was different in the thinner and thicker portions of the tube. Both studies assumed that this variable-thickness deformation could be modeled as if it were locally one-dimensional simple shear, involving only the coordinate along the tube axis, and as quasi-static and adiabatic, so that dynamical effects and heat conduction were neglected. Both papers also considered constitutive models for plastic flow which included strain and strain-rate hardening and thermal softening. The computational results in both studies indicated that the strain localized in the thinner, weaker part of the tube, once the load-displacement curve for the simulation changed from strain-hardening to strain-softening. Related computational results, in which heat conduction was also included, were reported by Shawki, *et al.* (1983) and Clifton, *et al.* (1984).

In Wright and Walter (1987), an analysis was given for the case of a strain-rate hardening and thermal softening material, so that strain-hardening effects were neglected. The deformation was treated as symmetric one-dimensional shearing of a thin layer with thermally insulated boundaries, and no variation in layer thickness was assumed. Instead, the problem was treated as homogeneous simple shear with a small, symmetric perturbation in temperature, so that the calculated deformation also localized in the mid-section of the shear layer. Because they assumed the shear layer had uniform thickness, *i.e.*, that any thickness perturbations were a higher-order effect which could be ignored, Wright and Walter observed that the stress remained homogeneous in the spatial coordinate throughout their calculations, which is in strong contrast with the results reported by Litonski, and by Molinari and Clifton. Wright and Walter used a numerical method which allowed them to compute long enough in time to be able to study the late stages of the formation of a single shear band at high strain rate. Their numerical calculations, which also included heat transport by conduction, indicated that, after a rapid transition to a localized deformation pattern in the mid-section of the shear layer, the strain rate became time-independent, while the temperature continued to increase and the stress continued to decrease, but both at a lower rate than before. Based on these observations, Wright and Walter gave an asymptotic description of what they called the late-stage shear band morphology, which they found to be in good agreement with their calculations. Additional asymptotic work in connection with this approach to modeling shear band evolution was given by Wright (1989). Related computational results, in which strain hardening effects were also included, were reported by Batra (1987) and by Batra and Kim (1988).

In contrast to the adiabatic temperature boundary conditions used in the studies just cited, Wright (1987) took a different approach to the late-time behavior of shear band formation. He assumed that the temperature boundary conditions were isothermal, and that eventually a saturation effect occurred in work-hardening, with the result that the material ceased to strain-harden. In this case, he showed that the evolution terms in his one-dimensional model equations for the deformation could be set equal to zero, with the result that stress, velocity, and temperature became independent of the time. The temperature boundary conditions forced the reference solution to be inhomogeneous. More recently, Chen, *et al.* (1989) studied the stability of this late-stage steady shearing morphology. Since fracture is often observed to occur during this late-stage deformation in the high strain rate torsion test (see, *e.g.*, Hartley, *et al.* (1987), Marchand and Duffy (1988)), it follows that, beyond a certain stage, the deformation process can no

longer be modeled as one-dimensional, and none of the above analyses continues to be applicable.

The purpose of the present paper is to propose a different, nonsteady mechanism, which can account for the formation of a single adiabatic shear band in the experimental torsion tests cited above. The mechanism is derived using an asymptotics argument, in which it is assumed that thickness variations, as well as elastic and dynamic effects in the tube, can be ignored, so that the stress remains homogeneous once plastic flow begins. The argument also assumes that heat transfer by conduction takes place through the ends of the thin-walled tubular specimen, so that the reference deformation becomes inhomogeneous, as in the studies by Wright (1987) and Chen, *et al.* (1989). The present work is thus consistent with the opinion of Marchand and Duffy (1988), that the ends of the thin-walled tubes in their experiments were attached to heat sinks, and that the stress remained homogeneous, except very early and very late in the loading history. The asymptotics argument is supported by a numerical analysis, which also depends on a small initial inhomogeneity in temperature, as in the numerical study of Wright and Walter (1987). The proposed mechanism is rigid unloading from the ends of the thin-walled tube, once the deformation process becomes unstable. The analysis shows that the unloading is enhanced by heat conduction, even though, as will be shown in what follows, the dimensionless group of parameters corresponding to the thermal diffusivity of the high strain rate deformation process is only of the order of magnitude of 10^{-3} to 10^{-2} . As with the analyses cited above, this work is only intended to apply while the torsion test remains essentially one-dimensional.

In Sec. 2, a one-dimensional model of the high strain rate torsion test is derived, based on Wallace's (1981), (1985) development of thermoelastic-plastic flow, which assumes the plastic flow surface includes strain and strain-rate hardening, as well as thermal softening. The resulting mathematical model is closely related to the one studied computationally by Wright and Batra (1985) and Wright and Walter (1987), (1989). Then in Sec. 3, the strain localization mechanism is derived, using an asymptotics argument, based on the derivation in Sec. 2. In order to test this hypothetical localization mechanism, a specific Arrhenius type constitutive model for the plastic flow surface is derived in Sec. 4, using the data for HY-100 steel given in Marchand and Duffy (1988). In Sec. 5, the results are presented of some computer simulations of the model problem, based on the semi-discretization method of lines, which strongly support the proposed localization mechanism. Concluding remarks and a discussion of these results are given in the final section.

2. Approximate One-Dimensional Problem

Before it is deformed, suppose a tube of ductile metal has length $d = 2.5$ mm, uniform wall thickness $H = 0.4$ mm, and uniform circular cross-sectional radius $R_0 = 9.7$ mm from the tube axis to the midpoint of the wall, so that its initial dimensions correspond to those in the samples studied experimentally by Marchand and Duffy (1988). When such a thin-walled tube is loaded in torsion, it is assumed here that the subsequent evolution of the deformation process is governed by the model of thermodynamically irreversible, isotropically elastic, thermoelastic-plastic flow derived by Wallace (1985) (also see Wallace (1981)). This model consists of an initial-boundary-value problem on a finite time interval and a bounded spatial domain for the standard continuum mechanics partial differential equations of conservation of mass, momentum, and energy, coupled with constitutive evolution equations for the stress tensor, the entropy, and the temperature, along with the the Prandtl-Reuss-von Mises equations for plastic yield and flow, and Fourier's law for heat conduction.

It is well-known that, during a torsion test, small radial length changes occur in the tube, and without confinement, small axial length changes would occur as well. In addition, large shear strains induce a small mean compressive stress (see, *e.g.*, Shrivastava, *et al.* (1982)). At high strain rates, heat produced by plastic work causes thermal expansion of the material, inducing an additional small contribution to the mean compressive stress (see, *e.g.* Wallace (1985)). As is commonly done in analyzing experimental torsion test data on ductile metals (see, *e.g.*, McMeeking (1982), Shrivastava, *et al.* (1982), Hartley and Duffy (1985)), it is assumed here that these small effects can be ignored. In particular, let the position of the tube in the undeformed (Lagrangian) configuration be given by cylindrical polar coordinates (R, Θ, Z) , with its axis coincident with the Z -axis from $Z = 0$ to $Z = d$, and let the corresponding cylindrical polar coordinate system in the current (Eulerian) configuration be denoted by (r, θ, z) . Let $\xi(Z, t)$ denote the angle of twist per unit length relative to the end $Z = 0$ of the tube through which the ring of material at Z has been rotated by the torsional loading process, so that $\xi(Z, 0) = 0$. It is assumed that the point on the midwall of the tube initially at $\mathbf{P} = (R_0, \Theta, Z)$, $0 \leq \Theta < 2\pi$, $0 \leq Z \leq d$, is moved by the deformation at time t to the point $\mathbf{p} = (r, \theta, z)$, where

$$\begin{aligned} r &= R_0, \\ \theta &= \Theta + Z\xi(Z, t), \\ z &= Z \end{aligned} \tag{1}$$

(see Shrivastava, *et al.* (1982)). Also, the only nonzero components of the true (Cauchy) stress tensor referred to the current (r, θ, z) coordinates are assumed to be

$$\sigma\langle\theta z\rangle = \sigma\langle z\theta\rangle = \tau \quad (2)$$

(see McMeeking (1982)), where τ is related to the applied torque Γ by $\Gamma = 2\pi R_0^2 H \tau$ (see Hartley and Duffy (1985)), and angular brackets denote physical components of a tensor. Define the shear strain γ and strain rate $\dot{\gamma}$ by

$$\gamma = \frac{\partial}{\partial Z} [R_0 Z \xi(Z, t)], \quad \dot{\gamma} = \frac{\partial}{\partial Z} [R_0 Z \dot{\xi}(Z, t)], \quad (3)$$

where the dot denotes the material time derivative, $\dot{\xi} = D\xi/Dt$. When ξ is homogeneous in Z , the strain defined in (3) reduces to the geometrically intuitive formula $\gamma = R_0 \xi$ (see Shrivastava, *et al.* (1982)). The only nonzero components of the deformation rate tensor \mathbf{D} , referred to the current configuration, are assumed to be

$$D\langle\theta z\rangle = D\langle z\theta\rangle = \frac{1}{2} \dot{\gamma} \quad (4)$$

(see McMeeking (1982), Shrivastava, *et al.* (1982)). While the assumptions (1), (2), and (4) are not consistent for large shear strains without making some additional approximations (see Shrivastava, *et al.* (1982)), it will be shown in what follows that they lead to a consistent mathematical model. An immediate consequence of either assumption (1) or (4) is that the deformation is volume-preserving. As a result, the mass density ρ , originally assumed to be homogeneous throughout the specimen, remains constant, so that the equation of conservation of mass is trivially satisfied (see Wallace (1985)).

The measure of deformation of most interest during the first two stages of the experiments of Marchand and Duffy (1988) is the twist $s(Z, t)$ at time t undergone by the circular ring of material in the tube labeled by the Lagrangian axial coordinate Z , since this is the variable which determines the instantaneous location of each of the grid lines etched on the tube prior to a test, as discussed in the Introduction. By inspection, for the simplified deformation assumed here, this is the arclength from $\mathbf{p}(Z, 0) = \mathbf{P}$ to $\mathbf{p}(Z, t)$, so that

$$s(Z, t) = R_0 Z \xi(Z, t). \quad (5)$$

The only nonzero component of the velocity \mathbf{v} associated with the map (1) is the angular speed $v = v\langle\theta\rangle$, where

$$v = R_0 Z \dot{\xi}. \quad (6)$$

From the definitions (5) and (6), it follows that the twist s and the angular speed v are related by

$$\frac{\partial s}{\partial t}(Z, t) = v(Z, t). \quad (7)$$

By (1) and (2), the equation of conservation of linear momentum reduces to a scalar equation in mixed Lagrangian-Eulerian form (see Wallace (1985)),

$$\rho \frac{\partial v}{\partial t}(Z, t) = \frac{\partial \tau}{\partial z}(z, t). \quad (8)$$

Since $z = Z$, it follows that, for a general function $f(Z, t)$, $f(Z, t) = f(z, t)$, so that the material time derivative equals the spatial time derivative,

$$\dot{f} = \frac{Df}{Dt} = \frac{\partial f}{\partial t}(Z, t) = \frac{\partial f}{\partial t}(z, t), \quad (9)$$

and trivially,

$$\frac{\partial f}{\partial z}(z, t) = \frac{\partial f}{\partial Z}(Z, t). \quad (10)$$

By (10), conservation of linear momentum (8) can be written in the purely Lagrangian form

$$\rho \frac{\partial v}{\partial t}(Z, t) = \frac{\partial \tau}{\partial Z}(Z, t). \quad (11)$$

The stress levels under consideration here are assumed to be much smaller than the elastic moduli, so the standard assumption will be made that the deformation rate \mathbf{D} in the current configuration can be decomposed into a sum of elastic and plastic contributions (see, *e.g.*, McMeeking (1982), Wallace (1985)), $\mathbf{D} = \mathbf{D}^e + \mathbf{D}^p$, so that

$$\dot{\gamma} = \dot{\gamma}^e + \dot{\gamma}^p. \quad (12)$$

It follows from (3) that the local twist rate of the tube $v = R_0 Z \dot{\xi}$ and the local strain rate $\dot{\gamma} = \partial (R_0 Z \dot{\xi}) / \partial Z$ are related by

$$\dot{\gamma} = \frac{\partial v}{\partial Z}. \quad (13)$$

Because of the assumptions (1) and (2), and the compatibility equation (13), the thermoelastic equations for the evolution of \mathbf{D}^e reduce to the scalar equation

$$\frac{\partial \tau}{\partial t} = G \dot{\gamma}^e = G \left(\frac{\partial v}{\partial Z} - \dot{\gamma}^p \right) \quad (14)$$

(see Wallace (1985)), where G is the shear modulus of the material, which is assumed to be a constant.

The Prandtl-Reuss constitutive approximation is (see Wallace (1985))

$$\mathbf{D}^P = \frac{3\boldsymbol{\sigma}'}{4\bar{\sigma}} \dot{\psi}, \quad (15)$$

where $\dot{\psi}$ is the effective plastic strain rate (see Shrivastava, *et al.* (1982)). The scalar variable $\bar{\sigma}$ denotes the effective shear stress, defined by

$$\bar{\sigma} = \sqrt{\frac{3}{4} S_2}, \quad (16)$$

where $S_2 = \frac{1}{2} \text{tr}(\boldsymbol{\sigma}'\boldsymbol{\sigma}')$ is the second rotational invariant of the deviator $\boldsymbol{\sigma}'$ of the Cauchy stress tensor $\boldsymbol{\sigma}$, defined by $\boldsymbol{\sigma}' = \boldsymbol{\sigma} - \frac{1}{3} \text{tr}(\boldsymbol{\sigma}) \mathbf{I}$. In the approximation under consideration here, $\boldsymbol{\sigma}' = \boldsymbol{\sigma}$. It follows that

$$\bar{\sigma} = \frac{\sqrt{3}}{2} \tau. \quad (17)$$

Using (12) and (17), the Prandtl-Reuss approximation (15) reduces to the scalar form

$$\dot{\gamma}^P = \sqrt{3} \dot{\psi}(Z, t). \quad (18)$$

The assumption (4) reduces the equation in Wallace (1985) for the evolution of absolute temperature T in the tube to

$$C \frac{\partial T}{\partial t}(Z, t) = T(Z, t) \frac{\partial S}{\partial t}(Z, t), \quad (19)$$

where C is the heat capacity at constant volume, and S is the specific entropy, *i.e.*, the entropy per unit mass. The equation for entropy production at a material point and a given time is given in Wallace (1985) in incremental form by

$$\rho T dS = \rho dQ + 2\bar{\sigma} d\psi, \quad (20)$$

where Q is the quantity of heat per unit mass, and $d\psi$ is the effective plastic strain increment. The plastic work W^P is defined incrementally by $dW^P = 2V\bar{\sigma} d\psi$, where V is the specific volume, $V = 1/\rho$. In (20), all of the plastic work W^P is assumed to be converted into heat, although it is known that a small percentage of this work goes into metallurgical changes in the material (Farren and Taylor

(1925)). Wallace (1981), (1985) argued that (20) is a good approximation which simplifies the thermoelastic theory. The continuity equation for heat transport is assumed to take the one-dimensional form

$$\rho \frac{\partial Q}{\partial t}(Z, t) = -\frac{\partial J}{\partial z}(z, t), \quad (21)$$

where J is the heat flux, and Fourier's law for heat transport is assumed to take the one-dimensional form $J(z, t) = -\kappa \partial T(z, t)/\partial z$, where κ is the thermal conductivity of the material, which is assumed here to be constant. Using (10) again, and substituting for $\bar{\sigma}$ and $\dot{\psi}$ using (17) and (18), it then follows that the equation for the evolution of the absolute temperature is given in Lagrangian form by

$$\rho C \frac{\partial T}{\partial t}(Z, t) = \kappa \frac{\partial^2 T}{\partial Z^2}(Z, t) + \tau(Z, t) \dot{\gamma}^p(Z, t). \quad (22)$$

The criterion for when plastic flow occurs, *i.e.*, for when $\dot{\psi} > 0$, is determined by a generalization of the von Mises yield criterion. Wallace (1985) generalized this criterion to a flow surface, such that

$$\bar{\sigma} = k(\psi, \dot{\psi}, V, S) \quad (23)$$

anywhere in the material where plastic flow is taking place. This allows for strain hardening, a strain-rate effect, and a dependence on the thermoelastic state (V, S). In the approximation used here, the specific volume V does not change, and by (19), the specific entropy S is a function of the temperature T . By (17) and (18), therefore, the von Mises flow surface (23) can be written in the form

$$\tau = K(\gamma^p, \dot{\gamma}^p, T). \quad (24)$$

It is assumed that $\partial K/\partial \dot{\gamma}^p > 0$, so that (24) can be inverted and written in the form

$$\dot{\gamma}^p = \Phi(\tau, \gamma^p, T). \quad (25)$$

The criterion for whether or not plastic flow takes place at a given material point at a given time is then given by

$$\dot{\gamma}^p = \begin{cases} \Phi(\tau, \gamma^p, T) & \text{if } \tau = K(\gamma^p, \dot{\gamma}^p, T), \\ 0 & \text{if } \tau < K(\gamma^p, 0, T). \end{cases} \quad (26)$$

For each fixed value of the angular material variable Θ , the mathematical model has been reduced to a set of five evolution equations in one material variable,

consisting of an equation for the total twist (7), a scalar equation for conservation of momentum (11), an equation for the evolution of the stress (14), an equation for the evolution of the temperature field in the axial direction of the tube (22), and an equation for the evolution of the plastic strain (26). Thus, the assumptions (1), (2), and (4) have led to a highly simplified model of the dynamic torsion problem, by allowing a reduction in the number of material coordinates on which the deformation depends, and by eliminating most of the physics which must be retained when thermoelastic effects are significant. To complete the specification of the mathematical model of the torsion test, boundary and initial conditions must be given, and a model for the flow surface (24) or (25) is required. As discussed in the Introduction, in most of the computer simulations to date of shear band formation, the boundary conditions on the temperature have been assumed to be adiabatic, *i.e.*, no heat flux through the boundaries, $\partial T(0, t)/\partial Z = \partial T(d, t)/\partial Z = 0$. It is assumed here, however, that the two ends of the thin-walled tube are constant-temperature heat sinks,

$$T(0, t) = T_L, \quad T(d, t) = T_R. \quad (27)$$

For the time being, it is assumed that $T_L = T_R = T_0$, where $T_0 = 300$ K denotes an approximate value of room temperature.

It follows from the expression for the velocity component in the θ -direction (6) that one boundary condition must be

$$v(0, t) = 0, \quad (28)$$

so that it is not appropriate to specify a boundary condition on the stress at $Z = 0$. The remaining boundary condition is that the rate of twist $R_0 Z \dot{\xi}$ of the end of the tube corresponding to $Z = d$ is constant. This corresponds approximately to the test conditions described in Costin, *et al.* (1979), Hartley, *et al.* (1987), and Marchand and Duffy (1988). By (6), this is equivalent to the constant-velocity boundary condition

$$v(d, t) = v_0, \quad (29)$$

where v_0/d is equal to a constant specified strain rate $\dot{\gamma}_0$ corresponding to a dynamic torsion test, assumed here to satisfy $\dot{\gamma}_0 = 100$ to 1600 s⁻¹. The model for the flow surface will be discussed in Sec. 4, and initial conditions will be discussed in Sec. 5. Before turning to these topics, the hypothesis for strain localization based on the model derived above will be discussed in the next section.

3. A Mechanism for Strain Localization

The equations (7), (11), (14), (22), (26), and the boundary conditions (27)-(29) can be scaled and nondimensionalized as follows. Let $\hat{Z} = Z/d$, $\hat{t} = \dot{\gamma}_0 t$, $\hat{s} = s/d$, $\hat{v} = v/v_0 = v/(\dot{\gamma}_0 d)$, $\hat{\tau} = \tau/\tau_0$, $\hat{T} = (T - T_0)/T_0$, $\hat{\gamma}^p = \gamma^p$ (the plastic strain is already dimensionless and can become the order of magnitude of one in a torsion test), $\hat{\Phi}(\hat{\tau}, \hat{\gamma}^p, \hat{T}) = \Phi(\tau, \gamma^p, T)/\dot{\gamma}_0$, and $\hat{K}(\hat{\gamma}^p, \dot{\hat{\gamma}}^p, \hat{T}) = K(\gamma^p, \dot{\gamma}^p, T)/\tau_0$. Dropping the hats over the variables, the resulting equations are

$$\begin{aligned}
 \frac{\partial s}{\partial t} &= v, \\
 \phi \frac{\partial v}{\partial t} &= \frac{\partial \tau}{\partial Z}, \\
 \zeta \frac{\partial \tau}{\partial t} &= \frac{\partial v}{\partial Z} - \Phi(\tau, \gamma^p, T), \\
 \frac{\partial T}{\partial t} &= \lambda \frac{\partial^2 T}{\partial Z^2} + \mu \tau \Phi(\tau, \gamma^p, T), \\
 \frac{\partial \gamma^p}{\partial t} &= \Phi(\tau, \gamma^p, T),
 \end{aligned} \tag{30}$$

when plastic flow is occurring, so that $\tau = K(\gamma^p, \dot{\gamma}^p, T)$ and $\dot{\gamma}^p > 0$. When the material is unloading, so that $\tau < K(\gamma^p, 0, T)$ and $\dot{\gamma}^p = 0$, the resulting equations are the same, except that $\Phi = 0$. The boundary conditions become

$$v(0, t) = 0, \quad v(1, t) = 1, \tag{31}$$

and

$$T(0, t) = 0, \quad T(1, t) = 0. \tag{32}$$

The dimensionless groups of parameters ζ, ϕ, λ , and μ are defined by

$$\zeta = \frac{\tau_0}{G}, \quad \phi = \frac{\tau_0}{\rho \dot{\gamma}_0^2 d^2}, \quad \lambda = \frac{\kappa}{\dot{\gamma}_0 d^2}, \quad \mu = \frac{\tau_0}{\rho C T_0}. \tag{33}$$

The shear modulus G for the structural steel HY-100 is assumed to be the handbook value for iron of 81 GPa. As discussed at the end of the preceding section, the range of strain rates assumed here is given by $\dot{\gamma}_0 = 100$ to 1600 s^{-1} , and the tests are assumed to take place at room temperature, $T_0 = 300 \text{ K}$. The length scale d is the tube gauge length, $d = 2.5 \text{ mm}$. The stress scale τ_0 is taken to be the stress level which gives the yield stress τ_y when the strain equals the yield

strain γ_y , assuming the material behaves according to a power-law hardening rule for small strain, *i.e.*, in dimensional form, $\tau = \tau_0 \gamma^n$, where

$$\tau_0 = \tau_y \gamma_y^{-n}. \quad (34)$$

The values chosen here for the parameters on the right-hand side in (34) are those reported by Marchand and Duffy (1988) for high strain-rate tests on HY-100 steel, $\tau_y = 463$ MPa, $\gamma_y = 0.012$, and $n = 0.107$, which give a value for the stress scale of $\tau_0 = 743.2$ MPa. The density scale ρ is taken to be the typical value for steel of 7800 kg/m³. The values taken for the heat capacity C and the thermal conductivity κ are given in turn by the typical values for iron of 500 J/(kg K) and 54 W/(m K). These parameter values yield orders of magnitude for the dimensionless groups (33) of $\zeta \approx 10^{-2}$, $\phi \approx 10^{-6}$ to 10^{-4} , $\lambda \approx 10^{-3}$ to 10^{-2} , and $\mu \approx 10^0$.

The smallness of the stress, inertia, and thermal diffusivity coefficients, ζ , ϕ , and λ , suggests that some approximations in addition to (1), (2), and (4) may be possible. For example, in Burns (1985), the case $\zeta \rightarrow 0$, $\phi \rightarrow 0$, $\lambda \rightarrow 0$ was discussed for adiabatic temperature boundary conditions. However, for the isothermal heat-sink boundary conditions (32) considered here, the limit $\lambda \rightarrow 0$ is clearly inappropriate, since heat conduction must be significant, at least near the two ends of the thin-walled tube, once the material begins to heat up during plastic deformation, in order to maintain the boundary temperature. This provides a mechanism for inhomogeneous deformation to evolve, as follows.

Assume that initially, $v(Z, 0) = Z$ and $T(Z, 0) = 0$, so that the deformation starts out homogeneous in strain and temperature. Consider the plastic flow surface $\tau = K(\gamma, \dot{\gamma}, T)$, which is assumed to satisfy the conditions

$$\partial K / \partial \gamma > 0, \quad 1 \gg \partial K / \partial \dot{\gamma} > 0, \quad \partial K / \partial T < 0, \quad (35)$$

so that the material strain hardens, has a small strain-rate effect (which is true for HY-100 steel; see Marchand and Duffy (1988)), and thermal softens. For torsion at constant strain rate and adiabatic temperature boundary conditions, a material which behaves according to such a model will harden initially, so that the stress will increase with increasing strain. If the deformation takes place at a high enough rate of strain, then eventually the material will begin to soften, with the stress decreasing with increasing strain (see Burns (1985), (1989)). While the deformation will then be unstable, in the absence of significant perturbations, it should still remain macroscopically homogeneous. With isothermal boundary conditions, on the other hand, if the torsion test is performed at a high enough

strain rate, then even with a small thermal diffusivity coefficient, the material near the tube ends will always be at a lower temperature than that near the mid-section of the tube. Thus, if the flow surface $\dot{\gamma}^p = \Phi(\tau, \gamma^p, T)$ has the property that $\partial\Phi/\partial T > 0$, so that the plastic strain rate increases with temperature, the accumulated plastic strain will also be less near the isothermal tube ends, so that the deformation will necessarily become inhomogeneous, even during the stable strain-hardening phase of the loading history.

Now, suppose it is valid to neglect the elastic shear strain beyond the yield strain γ_y , *i.e.*, suppose it is valid to take the asymptotic limit $\zeta \rightarrow 0$, so that, to a good approximation, the total strain γ equals the plastic strain γ^p , as is often done in interpreting data from the torsion test (see, *e.g.*, McMeeking (1982), Shrivastava, *et al.* (1982), Hartley and Duffy (1985)). Also assume it is valid to take the so-called quasi-static limit, $\phi \rightarrow 0$. In this limit, conservation of momentum, the second equation in (30), requires that the shear stress (2), and consequently the applied torque Γ , remain spatially uniform throughout the tube during the loading process. Then, once any material in the interior of the tube begins to soften, stress equilibration, $\partial\tau/\partial Z = 0$, will cause the cooler material near the tube ends, which will have accumulated less plastic strain than the central material if $\partial\Phi/\partial T > 0$, to be at a stress level which lies below its local flow surface value. This means that rigid unloading will occur near the ends, *i.e.*, $\dot{\gamma} = \dot{\gamma}^p = 0$, so that $\partial v/\partial Z = 0$ near the tube ends, by the third equation in (30).

As a result, plastic flow, and thus also heat production by plastic work, will cease in the outer portions of the tube. By the velocity boundary conditions (31), this means that a rigid-plastic unloading boundary, corresponding to regions of constant rate of twist, given by $v = 0$ on the left and $v = 1$ on the right, will move in towards the mid-section of the tube. How rapidly this free boundary moves inward will depend upon how rapidly the stress drops, which in turn will depend on how rapidly the local temperature increases, since $\partial K/\partial T < 0$. The rate of temperature increase will depend upon the result of a competition between the heat production term, $\mu\tau\dot{\gamma}$, and the heat transport term, which is the product of the dimensionless thermal diffusivity parameter, λ , and the curvature of the temperature distribution, $\partial^2 T/\partial Z^2$.

Since λ is inversely proportional to the applied dimensional strain rate, while the dimensionless heat production parameter μ is independent of the strain rate, heat transport by conduction will be more important the lower the applied strain rate. If λ is sufficiently small, *i.e.*, if the strain rate is sufficiently large, then the material will soften more rapidly than heat will be conducted away, and there will

not be enough time for any curvature in the temperature field near the mid-section of the tube to evolve. In this case, the deformation will not localize, even though it will be inhomogeneous and unstable once the material begins to strain-soften. On the other hand, if the applied strain rate is small enough, so that λ is large enough, heat transfer from the hotter central portion of the tube to the cooler tube ends will cause some curvature to develop in the temperature distribution near the mid-section of the tube. Since the stress is assumed to be uniform throughout the tube, the region of higher temperature will also be a region of higher strain, since, by (35),

$$0 = \frac{\partial \tau}{\partial Z} \approx \frac{\partial K}{\partial \gamma} \frac{\partial \gamma}{\partial Z} + \frac{\partial K}{\partial T} \frac{\partial T}{\partial Z},$$

so that, again by (35), $\partial \gamma / \partial Z$ and $\partial T / \partial Z$ will normally have the same sign. Once the deformation becomes unstable, this curvature will quickly become more pronounced. Thus, in this case, even under initial conditions which are homogeneous in strain and temperature, the moving unloading boundary will cause regions of increasing plastic strain and temperature to localize around the mid-section of the tube. This provides a natural mechanism for catastrophic shear strain localization to occur.

In practice, however, it is likely that there will always be at least a slight inhomogeneity in the initial distribution of the temperature, created, for example, by the experimental loading conditions (see, *e.g.*, Hartley and Duffy (1985)). Before the deformation becomes unstable, this initial temperature distribution will be modified by heat conduction through the tube ends, which, as discussed above, will be more significant the lower the strain rate, and, also as discussed above, this temperature inhomogeneity will produce an inhomogeneity in the strain distribution in the tube (this could also be modified at early time by the deformation process; see Burns (1989)). Thus, in general, because of these inhomogeneities, the deformation should begin to localize away from the mid-section, in the region of largest strain and temperature, before the symmetrical localization mechanism just described would have a chance to take place. By the same mechanism of runaway of plastic strain coupled with rigid unloading due to uniform stress softening, as discussed above for the symmetric case, a single shear band will then begin to form in the hottest local region once the material begins to soften. Depending on the size of the dimensionless thermal diffusivity parameter, which varies inversely with the strain rate, the band may then subsequently become narrower as more and more material surrounding the region of localization unloads, or it may widen due to heat transfer by conduction, aided by the fact that the tube ends will be

heat sinks. A computational study of this hypothetical strain localization mechanism will be presented in Sec. 5. In the next section, the specific flow surface model derived for the computations will be described.

4. Plastic Flow Surface Model

Suppose that strain localization into a single shear band will occur during a computer simulation by the moving boundary mechanism discussed in the preceding section. Then, as they stand, the two sets of equations defined by (30) and the yield criterion (26) will be difficult to treat numerically, because once the deformation becomes unstable, there will be a growing region near each tube boundary where the “rigid” set of equations, corresponding to $\dot{\gamma}^P = 0$, applies, and a shrinking central region where the “plastic” set of equations, corresponding to $\dot{\gamma}^P > 0$, applies, and these regions will be separated by rapidly steepening strain and temperature gradients. In order to make the computational problem more tractable, an Arrhenius model of the flow surface was chosen, which allowed the three hypothetical regimes determined by (30) and (26) to be combined into a single regime throughout the tube. This was done by eliminating the rigid unloading behavior, $\dot{\gamma}^P = 0$, and replacing it by an “effective” unloading, $\dot{\gamma}^P \approx 0$, thus allowing for a uniform numerical treatment of the problem, irrespective of whether or not plastic flow was taking place.

The phenomenological plastic flow surface for Φ was assumed to be given in terms of dimensional variables by

$$\dot{\gamma}^P = \dot{\gamma}_r \exp\left(-\frac{\Delta H(\tau)}{kT}\right) \quad (36)$$

(see *e.g.*, Kocks *et al.* (1975), Estrin and Kubin (1980)), where $\Delta H(\tau)$ is the activation enthalpy for the plastic deformation process, k is Boltzmann’s constant, T is the dimensional temperature, and $\dot{\gamma}_r$ is a term which was assumed to be constant and defined below. It was assumed that $\Delta H(\tau)$ could be linearized about the reference value of the flow stress, $\tau = \tau_0$, so that

$$\Delta H(\tau) \approx \Delta H(\tau_0) - \Delta V (\tau - \tau_0), \quad (37)$$

where $\Delta V = -\partial(\Delta H)/\partial\tau|_{\tau=\tau_0}$ is the apparent activation area Δa times the magnitude b of the Burgers vector \mathbf{b} , so that it has the dimensions of a volume. This approximation is probably not accurate for the large changes in the shear

stress τ which have been observed in the dynamic torsion test, but it did provide enough simplification of the Arrhenius model (36) so that it could be used as a phenomenological constitutive model for the plastic flow surface, based on the experimental data given by Marchand and Duffy (1988). The pre-exponential term $\dot{\gamma}_r$ was assumed to be given in terms of the constant reference conditions τ_0 , $\dot{\gamma}_0$, and T_0 by

$$\dot{\gamma}_r = \dot{\gamma}_0 \exp\left(\frac{\Delta H(\tau_0)}{kT_0}\right). \quad (38)$$

To account for strain hardening, the linear approximation (37) to the activation enthalpy was modified in the following way: Assume the strain-hardening behavior follows the power-law rule $\tau = \tau_r(\gamma^p) = \tau_0(\gamma_y + \gamma^p)^n$, where γ_y , τ_0 , and n have been defined and given numerical values in the preceding section. Then the constant reference stress τ_0 in the last term in (37) was assumed to be replaced by this power-law rule, so that, in modified approximate form, the constitutive equation for the flow stress is given by

$$\dot{\gamma}^p = \dot{\gamma}_r \exp\left\{-\frac{\Delta H(\tau_0) - \Delta V[\tau - \tau_r(\gamma^p)]}{kT}\right\}. \quad (39)$$

Rewriting (39) using the dimensionless variables defined in the preceding section, the linearized Arrhenius model has the form

$$\dot{\gamma}^p = \Phi(\tau, \gamma^p, T) = \exp\left\{\frac{\beta T + \alpha[\tau - \tau_r(\gamma^p)]}{1 + T}\right\}, \quad (40)$$

so that it introduces four new dimensionless groups of parameters. Two of these are the yield strain γ_y and the strain-hardening exponent n , which have already been discussed above. The remaining two are a temperature coefficient β , where $\beta = \Delta H(\tau_0)/(kT_0)$, and a stress coefficient α , where $\alpha = \Delta V\tau_0/(kT_0)$. By (38), $\beta = \ln(\dot{\gamma}_r/\dot{\gamma}_0)$. Kocks *et al.* (1975, p. 243) gave the estimated bounds on β of $8 < \beta < 40$, where the upper bound corresponds to a strain rate of the order of magnitude of 10^2 . Since the order of magnitude of the strain rates in the present study was assumed to be 10^2 to 10^3 , a value of $\beta = 40$ was chosen for the temperature coefficient.

It was decided to fit the remaining parameter, α , by requiring that a homogeneous deformation of the thin-walled tube described in Sec. 2, at a constant dimensional strain rate of $\dot{\gamma}_0 = 1600 \text{ s}^{-1}$, with adiabatic temperature boundary conditions, attain its maximum stress at a homogeneous strain value of $\gamma_p = 0.25$,

corresponding to a typical strain value at which a stress maximum was observed by Marchand and Duffy (1988) in their experiments. The reasoning behind this choice of parameter value was that, since the dimensionless thermal diffusivity parameter λ is very small, heat transfer from the central portion of the tube to its boundaries should not be significant, *i.e.*, the deformation away from the boundaries should be adiabatic to a good approximation, and hence the central material should behave according to this homogeneous history, until it becomes unstable and gradients in strain and temperature become important. The approximate value of the stress coefficient determined in this way was found to be $\alpha = 55$, which gave a peak dimensional stress value of approximately 580 MPa, which is about 6% lower than the average of the peak stresses reported by Marchand and Duffy (1988, Table 3).

As a consistency check on the order of magnitude of α , first solve for τ as a function of the other variables in the constitutive equation (40), which is valid, since clearly $\partial\dot{\gamma}^p/\partial\tau > 0$. The result is

$$\tau = K(\gamma^p, \dot{\gamma}^p, T) = \tau_r(\gamma^p) + \frac{(1+T)}{\alpha} \ln \dot{\gamma}^p - \frac{\beta}{\alpha} T. \quad (41)$$

From this, it follows that the mean apparent strain-rate sensitivity parameter, $m = \partial\tau/\partial \ln \dot{\gamma}^p$ (see, *e.g.*, Eleiche (1981)), is given at constant temperature and plastic strain by $m = (1+T)/\alpha$. Thus, m is of the same order of magnitude as $1/\alpha \approx 10^{-2}$, which is the correct order of magnitude of m for low-carbon steel (Eleiche (1981)).

As another consistency check on the constitutive model, recall that a necessary requirement for the strain localization mechanism described in the preceding section to be possible is that the strain rate must increase with temperature, *i.e.*, that

$$\partial\dot{\gamma}^p/\partial T > 0 \quad (42)$$

in (40). By (40),

$$\frac{\partial\dot{\gamma}^p}{\partial T} = \frac{[\beta - \alpha(\tau - \tau_r)]}{(1+T)^2} \exp \left\{ \frac{\beta T + \alpha[\tau - \tau_r(\gamma^p)]}{1+T} \right\},$$

so if $\tau < \tau_r + \beta/\alpha$, the condition (42) will be satisfied. To verify this, notice that while plastic flow is taking place, the shear stress must lie on the flow surface (41). As long as the scaled, dimensionless plastic strain rate satisfies the inequality $0 < \dot{\gamma}^p < \exp \beta$, it is straightforward to check that $\tau < \tau_r + \beta/\alpha$. Since $\exp \beta$

is enormous, the condition (42) will be satisfied for any conceivable strain rate achievable in a torsion test.

The yield criterion (26) was replaced by the Arrhenius model (40), so that, computationally, the material always deformed in the plastic regime. Since α and β are relatively large coefficients of approximately the same order of magnitude, it was reasoned that this Arrhenius plastic flow model should behave computationally according to the following heuristic asymptotics argument. Define the small parameter ϵ by $\epsilon = 1/\alpha$. Then (40) can be written in the form

$$\dot{\gamma}^p = \exp \left\{ \frac{\nu T + [\tau - \tau_r(\gamma^p)]}{\epsilon(1+T)} \right\}, \quad (43)$$

where $\nu = \beta/\alpha \approx 1$ is assumed to be a similarity parameter which is independent of ϵ . Solving for τ as in (41),

$$\tau = \tau_r(\gamma^p) + \epsilon(1+T) \ln \dot{\gamma}^p - \nu T, \quad (44)$$

it follows that $\tau \approx \tau_r - \nu T$ as $\epsilon \rightarrow 0$, unless $\dot{\gamma}^p = O(\exp -1/\epsilon)$. By (43), this latter condition will be satisfied when τ drops below $\tau_r - \nu T$; to be more precise, the condition is satisfied when $[\tau - (\tau_r - \nu T)] / (1+T)$ is negative and $O(1)$ in ϵ . When this condition is satisfied, clearly $0 < \dot{\gamma}^p \ll 1$. According to the scenario in Sec. 3 above, this corresponds to rigid unloading due to stress equilibration. Thus, the Arrhenius model (40), which should apply with no difficulty in the plastic flow regime, should also give a good approximation to the rigid unloading behavior $\dot{\gamma}^p = 0$, which will propagate inward from the tube ends, if the hypothesis of the preceding section is valid. A computational study of this hypothesis will be discussed in the next section.

5. Computational Results

To study the validity of the strain localization mechanism proposed in Sec. 3, the system of five partial differential equations (PDE's) (30), with the Arrhenius plastic flow model (40) (*i.e.*, with no provision for unloading), and the boundary conditions (31), were solved numerically using the semi-discretization method of lines (see, *e.g.*, Smith (1985, Chap. 3)). As used here, the basic idea of this method is to discretize the right-hand sides of the PDE's uniformly in Z using a centered finite-difference method, taking into account the boundary conditions, resulting in a (potentially very large) coupled system of ordinary differential equations

(ODE's). The system of ODE's is then solved using a separate numerical method, so that advantage can be taken of the sophisticated mathematical software which is currently available for initial-value problems. Because the time derivatives of two of the equations in (30) are multiplied by small parameters, and because the temperature evolution equation is parabolic, the resulting system of ODE's can be very stiff (see Gear (1971)), especially if the spatial discretization interval is small (see Smith (1985)). For this reason, the public-domain method of lines software MOL1D (Hyman (1979)) was chosen for the computer simulations. This software incorporates Hindmarsh's (1975) version of the backward-difference method of Gear (1971) for stiff ODE's. Wright and Walter (1987), (1989), and Batra and Kim (1988) used versions of the method of lines based on Gear's method and a semi-discretization using the finite-element method.

The initial time in the calculations was simplified by making the assumption that, in dimensional variables, $\tau = \tau_y$ and $\gamma = 0$ at $t = 0$. Thus, the small initial elastic range of the material behavior was ignored, since there was no reason to believe that the constitutive model (40) provides a good approximation to this early-time behavior, anyway. The calculations were all run on a uniform spatial grid of 101 points, so that the mesh width was $25 \mu\text{m}$. The first calculations which will be discussed were done to test the hypothetical symmetrical localization mechanism described in Sec. 3. For the first calculation, it was assumed that the applied dimensional strain rate was $\dot{\gamma}_0 = 1600 \text{ s}^{-1}$. To two significant figures, the dimensionless parameters in the problem were then as follows, $\alpha = 55$, $\beta = 40$, $\zeta = 0.92 \times 10^{-2}$, $\phi = 0.17 \times 10^{-3}$, $\lambda = 0.14 \times 10^{-2}$, $\mu = 0.64$. Also, the function τ_r was given by $\tau_r = (0.012 + \gamma^p)^n$, where $n = 0.107$. The initial twist, temperature, and plastic strain fields were assumed to be identically equal to zero; the initial stress was set equal to $(0.012)^n \approx 0.62$; and the initial velocity was assumed to increase linearly from 0 at $Z = 0$ to 1 at $Z = 1$, $v(Z, 0) = Z$, corresponding to a homogeneous initial strain rate of $\dot{\gamma} = 1$. Thus, in a deformation that remains homogeneous, $\gamma(Z, t) = t$, so the dimensionless time variable is the same as the homogeneous strain. The nominal strain in some of the figure labels refers to the twist at the right-hand end of the tube, $s(1, t) = [s(1, t) - s(0, t)]$, which is the dimensionless time, and is thus what the shear strain would equal under conditions of homogenous simple shear, with adiabatic boundary conditions in temperature. The results of this calculation are given in Fig. 1-2. The stress was found to remain homogeneous throughout the calculation, with its peak occurring at approximately $\gamma^p = 0.25$. In Fig. 2, the stress in the tube and the temperature in the hottest region of the tube are plotted. The

deformation became inhomogeneous, but the thermal diffusivity was too small, and numerical noise was insufficient, to cause catastrophic localization, once the process became unstable.

In the second calculation, the initial conditions were the same, but now it was assumed that the applied dimensional strain rate was $\dot{\gamma}_0 = 100 \text{ s}^{-1}$. Since the acceleration coefficient ϕ decreases as the square of the applied dimensional strain rate $\dot{\gamma}_0$, while the stress rate coefficient ζ remains unchanged, the semi-discretized PDE's became much stiffer numerically when $\dot{\gamma}_0$ was decreased, with the result that the calculation slowed down significantly once the stress began to soften, and it never ran to completion. Because of this, the parameter ϕ was then set back to the value corresponding to the higher strain rate of 1600 s^{-1} , while λ was kept at the 16 times larger value corresponding to $\dot{\gamma}_0 = 100 \text{ s}^{-1}$. Thus, this calculation can be interpreted as the second in a parameter study of the influence of the dimensionless thermal diffusivity on shear strain localization. If the asymptotic limits $\zeta \rightarrow 0$, $\phi \rightarrow 0$ assumed in Sec. 3 are valid, then this calculation should also provide an approximate model of the same experiment simulated in the first calculation, but at a lower strain rate. The results of this simulation are given in Fig. 3-4. The stress was once again found to remain homogeneous in Z throughout the calculation, with its peak occurring at approximately $\gamma^p = 0.25$. Also, from the graph of v vs. Z , it is clear that the assumptions $\zeta \rightarrow 0$, $\phi \rightarrow 0$, and the symmetric localization scenario hypothesized in Sec. 3 above, are supported by the calculation. Notice that the width of the shear band actually increased as the deformation progressed, once it began to localize, due to the large value of the thermal diffusivity. This also accounts for the crossing of the last few velocity curves in Fig. 3(b).

As discussed in the Introduction, Marchand and Duffy (1988) concluded that there were three stages of shear strain localization in their torsion tests. In the final stage, for a given axial location Z , the total twist was found to depend on the circumferential variable Θ , so there was no hope that the simple one-dimensional mathematical model derived here could simulate the observed late-time behavior. Keeping this in mind, the last calculations which will be discussed were some simulations of a typical test reported by Marchand and Duffy (1988), with numerical parameter values corresponding to $\dot{\gamma}_0 = 1600 \text{ s}^{-1}$, as in the first calculation described above, and initial conditions the same as well, except that, instead of a dimensionless homogeneous initial temperature of $T(Z, 0) = 0$, a small, constant temperature gradient was introduced. The reason for introducing the inhomogeneity this way was to study the effect on localization of heat transfer

by conduction through the tube ends. An alternative approach would have been to follow the procedure of Wright and Batra (1985), and subsequently others, who introduced an initial temperature perturbation which was symmetric, with a single maximum in the center. Under these conditions, with isothermal boundary conditions, the deformation would have been expected to localize in the mid-section of the tube, as in the second calculation described above.

In one of these simulations, the initial temperature distribution was set equal to $T(Z, 0) = Z/20$, and the right dimensionless boundary condition in temperature was set to be compatible with this, $T(1, 0) = 1/20$. Such an initial distribution gave a temperature difference of 15 C between the two ends of the thin-walled tube. While some inhomogeneity in the initial temperature due to the loading conditions is likely to have been present in the experiments, this assumed distribution was probably much too simplistic. The results of this calculation are shown in Fig. 5-6. The stress was found to remain homogeneous in Z until the end of the calculation, when small oscillations also appeared in the velocity, as shown in Fig. 5(b) & (e). These oscillations were probably due to the numerical method used, and are reminiscent of the oscillations which occur behind a shock wave in numerical simulations (see, *e.g.*, Richtmyer and Morton (1967)). Assuming this to be the correct explanation, the calculation again strongly supports the assumption that $\phi \rightarrow 0$. The regions of constant velocity propagating inwards from the two ends of the tube at late time also strongly support the rigid unloading hypothesis, *i.e.*, that $\zeta \rightarrow 0$. The results of this calculation also demonstrate that an initial local temperature maximum in the interior of the thin-walled tube is not a necessary requirement for catastrophic strain localization to occur during the torsion test.

From the plots of the temperature and plastic strain vs. Z in Fig. 5, it is clear that localization occurred between values of the strain of 0.35 and 0.40, which compares favorably with the 0.35 – 0.45 reported by Marchand and Duffy. The qualitative agreement between the calculated stress and temperature vs. nominal shear strain curves in Fig. 6 and the corresponding experimental curves in Marchand and Duffy (1988, Fig. 12 & 21) is also very encouraging. Also notice that, in Fig. 6, beyond a strain of about 0.40, the stress began to drop off more slowly. This does not agree with the experimental observations of Marchand and Duffy (1988, Fig. 12 & 21), that the stress continued to drop catastrophically. This is not surprising, because the experimentally observed deformation ceased to remain one-dimensional in this regime, and in some cases, it was observed to fracture. As discussed above, the present simulations cannot be expected to model these phenomena. At a time corresponding to a homogeneous strain of $\gamma = 0.45$, the shear

band covered less than two mesh widths, so that its width was somewhere between $25 - 50 \mu\text{m}$ wide. To resolve this width any finer would require doubling or tripling the mesh width, and was not done here. As it stands, however, this calculated band width compares favorably with the width measured by Marchand and Duffy during Stage III of about $20 \mu\text{m}$. At $\gamma = 0.45$, the corresponding dimensional temperature was calculated to be approximately 450 C . This is in good agreement with the measured values reported by Marchand and Duffy (1988, Table 5).

The same calculation was repeated, with the only changes that the initial temperature distribution was assumed to be $T(Z, 0) = Z/30$ and $T(Z, 0) = Z/100$, with compatible boundary conditions, so that the right end of the tube was initially 10 C and 3 C hotter than the left end. The main difference between these two calculations and the one with the 15 C initial temperature difference was that, in the latter two, localization occurred at respective nominal strains which were about 0.05 and 0.15 larger than in the former one. As a final observation, the shear band width was found to decrease with increasing strain in the latter three calculations, unlike the symmetric case in Fig. 3, due to the smallness of the dimensionless thermal diffusivity parameter.

6. Concluding Remarks and Discussion

An asymptotics argument has been given, which has led to the proposal of a new mechanism for strain localization in the high strain rate torsion test. The mechanism is an inwardly moving boundary of rigid unloading, once the deformation becomes unstable due to thermal softening, which isolates the material in the locally hottest region of the thin-walled tube. The argument has depended on the test remaining essentially one-dimensional until after catastrophic strain localization begins to occur; on the shear stress remaining in spatial equilibrium, and on the material behavior being rigid-thermoviscoplastic, once plastic flow begins; and on an outward flux of heat through the two ends of the thin-walled tube (it is not essential that the boundaries be held at a constant temperature; for example, T_R could vary with time). Numerical analysis, using the method of lines code of Hyman (1979), of a mathematical model of some of the experiments of Marchand and Duffy (1988), based on Wallace's (1980), (1985) irreversible thermodynamics model of thermoelastic-plastic flow, and a phenomenological Arrhenius model of HY-100 steel, based on Marchand and Duffy's data, have been shown to lend strong support to this hypothetical mechanism.

Because the rigid-thermoviscoplastic limit, $\zeta \rightarrow 0$, has been a necessary assumption for the localization mechanism described here, it would seem more natural to have made this assumption in Sec. 2. The reason it was not assumed in Sec. 2 that all elastic strains could be ignored is that the resulting system of PDE's was found to provide a much more difficult computational problem. The key to the application of the numerical method used here was the adoption of the system of evolution equations (30), along with the Arrhenius model (40) for the plastic flow surface, even in regions where classical plasticity theory says no plastic flow should take place. Also, as discussed in the preceding section, because the dimensionless parameter ϕ decreases as the square of the nominal strain rate, numerical simulation of a test at a strain rate of 500 s^{-1} became much more difficult to do, at least with the method used here, since ϕ was an order of magnitude smaller. For this reason, and because the material parameters are also different from those for HY-100 steel, no simulations of the lower strain rate tests on the mild steels 1018 CRS or 1020 HRS reported by Costin, *et al.* (1979), and Hartley, *et al.* (1987), have been discussed here.

As discussed in Sec. 4, the Arrhenius model used here (40) has been assumed to have the form $\dot{\gamma}^p = \exp[f(\tau, \gamma^p, T)/\epsilon T]$, where ϵ is a small dimensionless parameter. Because of this, it would be nice to connect the strain localization problem discussed here with some of the modeling of thermal explosions which has been done in the mathematical theory of combustion, using activation energy asymptotics (see, *e.g.*, Kapila (1983)). This does not appear to be possible, for the following reason. The limit $\zeta \rightarrow 0$ has been a necessary assumption for the localization scenario discussed above. Because of this, when plastic flow is occurring, as discussed in Sec. 4, the plastic strain rate does not grow like $\exp 1/\epsilon$, so that the temperature does not increase as rapidly as in a thermal explosion, *i.e.*, like the solution of

$$\dot{T} = \frac{\epsilon}{b} (1 + b - T) \exp\left(\frac{T - 1}{\epsilon T}\right), \quad T(0) = 1,$$

as $\epsilon \rightarrow 0$, for some positive constant b .

Finally, in connection with the assumed initial temperature distributions in some of the calculations discussed in the preceding section, it would be very interesting to see an experimental measurement of the early-time temperature distribution during a high strain rate torsion test, or a two-dimensional computational analysis of the test, similar to that done by Bertholf (1974) for the split-Hopkinson pressure bar system, which also includes the evolution of the temperature field.

Acknowledgments

It is a pleasure to acknowledge helpful conversations with R. C. Batra of the University of Missouri-Rolla, J. Duffy of Brown University, D. G. Lasseigne of Old Dominion University, P. H. Leo of the University of Minnesota, and T. W. Wright of the U. S. Army Ballistics Research Laboratory.

References

Batra, R. C., 1987, "The Initiation and Growth of, and the Interaction Among, Adiabatic Shear Bands in Simple and Dipolar Materials," *Int. J. Plasticity*, Vol. 3, pp. 75-89.

Batra, R. C., and Kim, C. H., 1988, "Adiabatic Shear Banding in Elastic-Viscoplastic Nonpolar and Dipolar Materials," to appear.

Bertholf, L. D., 1974, "Feasibility of Two-Dimensional Numerical Analysis of the Split-Hopkinson Pressure Bar System," *J. Appl. Mech.*, Vol. 41, pp. 137-144.

Burns, T. J., 1985, "Approximate Linear Stability Analysis of a Model of Adiabatic Shear Band Formation," *Quart. Appl. Math.*, Vol. 43, pp. 65-84.

Burns T. J., 1989, "Similarity and Bifurcation in Unstable Viscoplastic Shear," *SIAM J. Appl. Math.*, Vol. 49, pp. 314-329.

Chen, H. Tz., Malek-Madani, R., and Douglas, A. S., 1989, "An Asymptotic Stability Condition for Inhomogeneous Simple Shear," *Quart. Appl. Math.*, Vol. 47, pp. 247-262.

Clifton, R. J., Duffy, J., Hartley, K. A., and Shawki, T. G., 1984, "On Critical Conditions for Shear Band Formation at High Rates," *Scripta Metall.*, Vol. 18, pp. 443-448.

Costin, L. S., Crisman, E. E., Hawley, R. H., and Duffy, J., 1979, "On the Localisation of Plastic Flow in Mild Steel Tubes under Dynamic Torsional Loading," *Inst. Phys. Conf. Ser. No. 47*, Oxford, U.K., pp. 90-100.

Eleiche, A. M., 1981, "Strain-rate History and Temperature Effects on the Torsional-shear Behavior of a Mild Steel," *Experimental Mech.*, Vol. 21, pp. 285-294.

Estrin, Y., and Kubin, L. P., 1980, "Criterion for Thermomechanical Instability of Low Temperature Plastic Deformation," *Scripta Metall.*, Vol. 14, pp. 1359-1364.

Farren, W. S., and Taylor, G. I., 1925, "The Heat Developed during Plastic Extension of Metals," *Proc. Roy. Soc.*, Vol. A107, pp. 422-451.

Gear, C. W., 1971, *Numerical Initial Value Problems in Ordinary Differential Equations*, Prentice-Hall, Englewood Cliffs, N.J.

Hartley, K. A., and Duffy, J., 1985, "The Torsional Kolsky (Split-Hopkinson) Bar," *Metals Handbook*, Vol. 8, American Society for Metals, Metals Park, Oh., pp. 218-228.

Hartley, K. A., Duffy, J., and Hawley, R. H., 1987, "Measurement of the Temperature Profile During Shear Band Formation in Steels Deforming at High Strain Rates," *J. Mech. Phys. Solids*, Vol. 35, pp. 283-301.

Hindmarsh, A. C., 1975, *GEARB: Solution of Ordinary Differential Equations Having Banded Jacobian*, Lawrence Livermore National Laboratory Report UCID-30059, Rev. 1, Livermore, Ca.

Hyman, J. M., 1979, *MOL1D: A General Purpose Subroutine Package for the Numerical Solution of Partial Differential Equations*, Los Alamos National Laboratory Manual LA-7595-M, Los Alamos, N.M.

Kapila, A. K., 1983, *Asymptotic Treatment of Chemically Reacting Systems*, Pitman, Boston-London-Melbourne.

Kochs, U. F., Argon, A. S., and Ashby, M. F., 1975, *Thermodynamics and Kinetics of Slip*, Pergamon Press, Oxford, U.K.

Litonski, J., 1977, "Plastic Flow of a Tube under Adiabatic Torsion," *Bull. Acad. Polonaise Sci.*, Vol. 25, pp. 7-14.

Marchand, A., and Duffy, J., 1988, "An Experimental Study of the Formation Process of Adiabatic Shear Bands in a Structural Steel," *J. Mech. Phys. Solids*, Vol. 36, pp. 251-283.

McMeeking, R. M., 1982, "The Finite Strain Tension Torsion Test of a Thin-Walled Tube of Elastic-Plastic Material," *Int. J. Solids Structures*, Vol. 18, pp. 199-204.

Molinari, A., and Clifton, R. J., 1987, "Analytical Characterization of Shear Localization in Thermoviscoplastic Materials," *J. Appl. Mech.*, Vol. 54, pp. 806-812.

Richtmyer, R. D., and Morton, K. W., 1967, *Difference Methods for Initial-Value Problems*, Interscience, New York-London-Sydney.

Rogers, H. C., 1979, "Adiabatic Plastic Deformation," *Ann. Rev. Mat. Sci.*, Vol. 9, pp. 283-311.

Shawki, T. G., Clifton, R. J., and Majda, G., 1983, "Analysis of Shear Strain Localization in Rate Sensitive Materials," Technical Report DAAG-29-81-0121/3, Division of Engineering, Brown University, Providence, R.I.

Shrivastava, S. C., Jonas, J. J., and Canova, G., 1982, "Equivalent Strain in

Large Deformation Torsion Testing: Theoretical and Practical Considerations," *J. Mech. Phys. Solids*, Vol. 30, pp. 75-90.

Smith, G. D., 1985, *Numerical Solution of Partial Differential Equations: Finite Difference Methods*, Oxford University Press, Oxford, U.K.

Wallace, D. C., 1981, "Irreversible Thermodynamics of Flow in Solids," *Phys. Rev.*, Vol. B22, pp. 1477-1486.

Wallace, D. C., 1985, *Thermoelastic-Plastic Flow in Solids*, Los Alamos National Laboratory Report LA-10119, Los Alamos, N.M.

Wright, T. W., 1987, "Steady Shearing in a Viscoplastic Solid," *J. Mech. Phys. Solids*, Vol. 35, pp. 269-282.

Wright, T. W., 1989, "Approximate Analysis for the Formation of Adiabatic Shear Bands," to appear.

Wright, T. W., and Batra, R. C., 1985, "The Initiation and Growth of Adiabatic Shear Bands," *Int. J. Plasticity*, Vol. 1, pp. 205-212.

Wright, T. W., and Walter, J. W., 1987, "On Stress Collapse in Adiabatic Shear Bands," *J. Mech. Phys. Solids*, Vol. 35, pp. 701-720.

Wright, T. W., and Walter, J. W., 1989, "Adiabatic Shear Bands in One Dimension," U.S. Army Ballistics Research Laboratory Memorandum Report BRL-MR-3759, Aberdeen Proving Ground, Md., to appear in Proc. of 4th Oxford Conference on Mechanical Properties at High Rates of Strain.

Zener, C., and Hollomon, J. H., 1944, "Effect of Strain Rate Upon Plastic Flow of Steel," *J. Appl. Phys.*, Vol. 15, pp. 22-32.

Figure Captions

Figure 1. Plots of (a) twist, (b) twist rate, (c) temperature, and (d) plastic strain, for $\dot{\gamma}_0 = 1600 \text{ s}^{-1}$, as functions of the axial coordinate Z , for nominal strain values of 0.0–0.80, in increments of 0.10 (see text). No shear band was observed in this simulation. Note that $\gamma^P = t$ in the central portion of the tube until the deformation became unstable, with $\gamma^P > t$.

Figure 2. Plots of dimensionless stress (upper curve initially) and peak temperature (lower curve initially) vs. nominal strain taken from the calculation in Fig. 1. Note that the peak stress occurred at a strain of approximately 0.25.

Figure 3. Plots of (a) twist, (b) twist rate, (c) temperature, and (d) plastic strain, as functions of the axial coordinate Z , for nominal strain values of 0.0–0.80, in increments of 0.05. All parameters are the same as in Fig. 1, except that the value of λ was for a strain rate of $\dot{\gamma}_0 = 100 \text{ s}^{-1}$ (see text). A symmetric shear band was observed to form, supporting the localization mechanism discussed in Sec. 3. Note that the band widened with increasing strain due to the large thermal diffusivity λ .

Figure 4. Plots of dimensionless stress and peak temperature vs. nominal strain taken from the calculation in Fig. 3.

Figure 5. Plots of (a) twist, (b) twist rate, (c) temperature, and (d) plastic strain, for nominal strain values of 0.0–0.45, and (e) stress, for nominal strain values of 0.25–0.45, in increments of 0.05, as functions of the axial coordinate Z , for parameter values corresponding to a strain rate of $\dot{\gamma}_0 = 1600 \text{ s}^{-1}$. The initial temperature distribution was assumed to be $T(Z, 0) = Z/20$. An adiabatic shear band of 25–50 μm in width formed at a nominal strain of between 0.35–0.40. Note that there was no widening of the band with increasing strain in this simulation.

Figure 6. Plots of stress and peak temperature vs. nominal strain, in dimensional variables, taken from the calculation in Fig. 5. The initial peak temperature was 42 C at the right-hand tube end. Notice the inflection points in the two graphs at about the time the shear band formed.

FIG. 1(a)

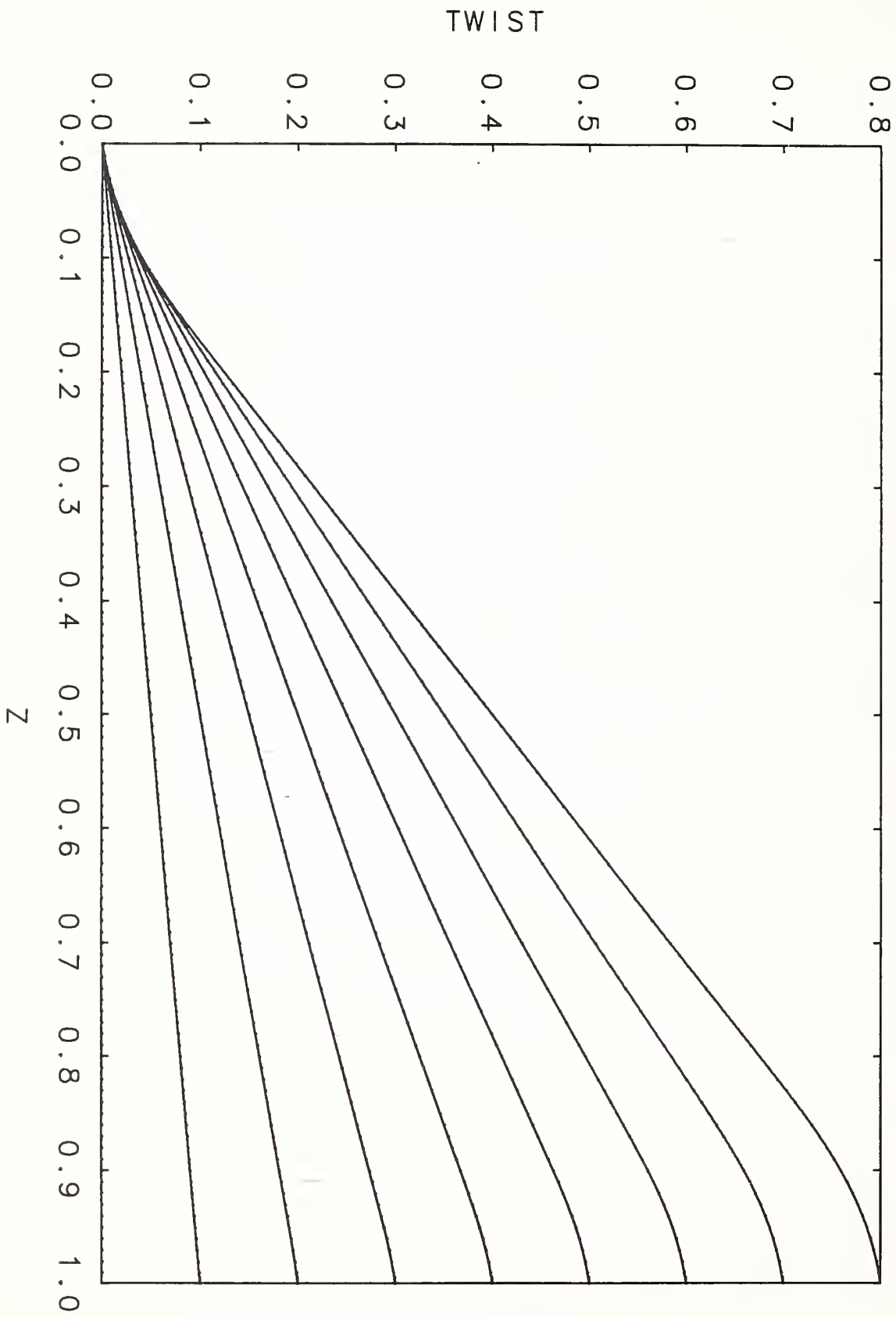


FIG. 1(b)

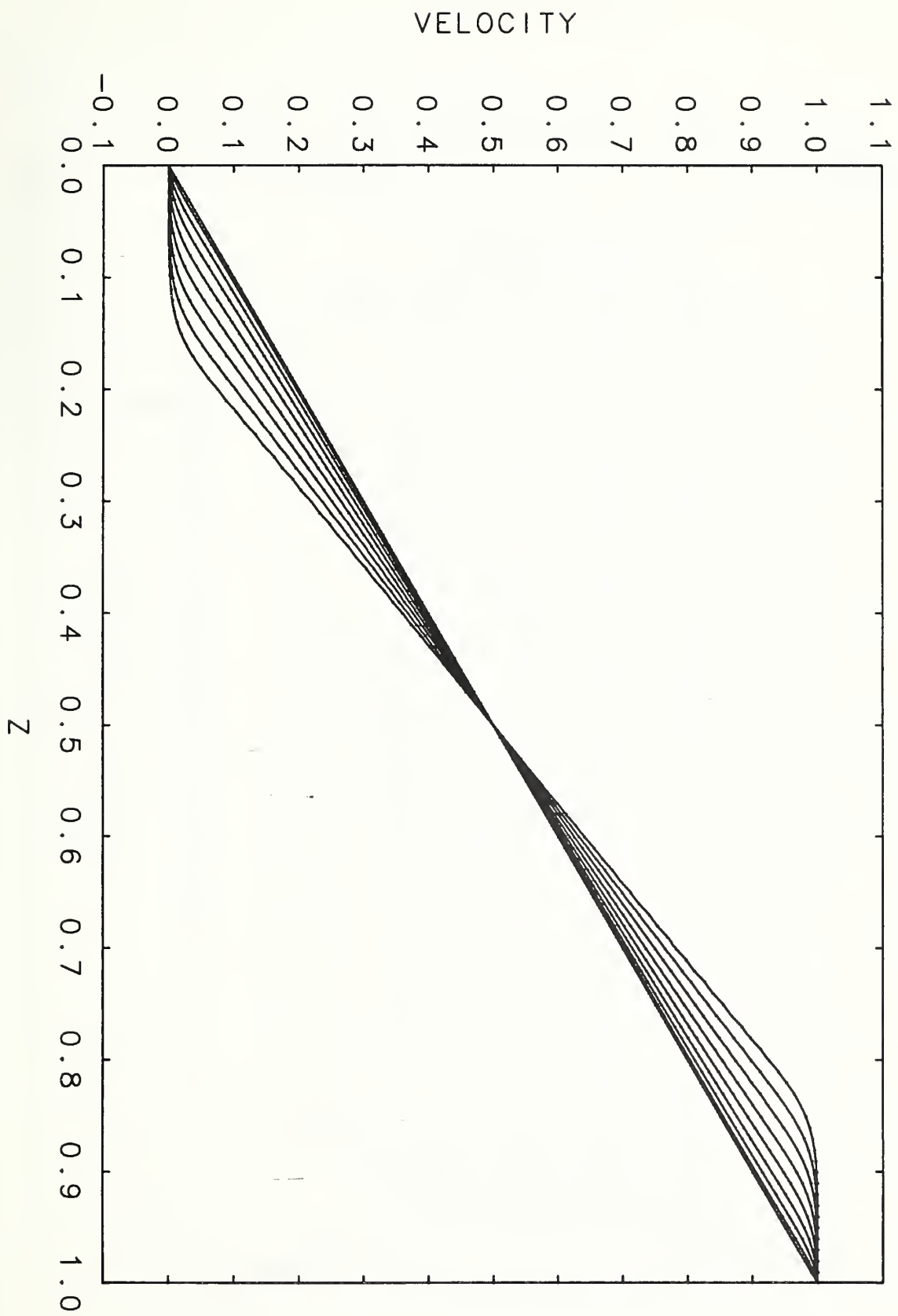


FIG. 1(c)

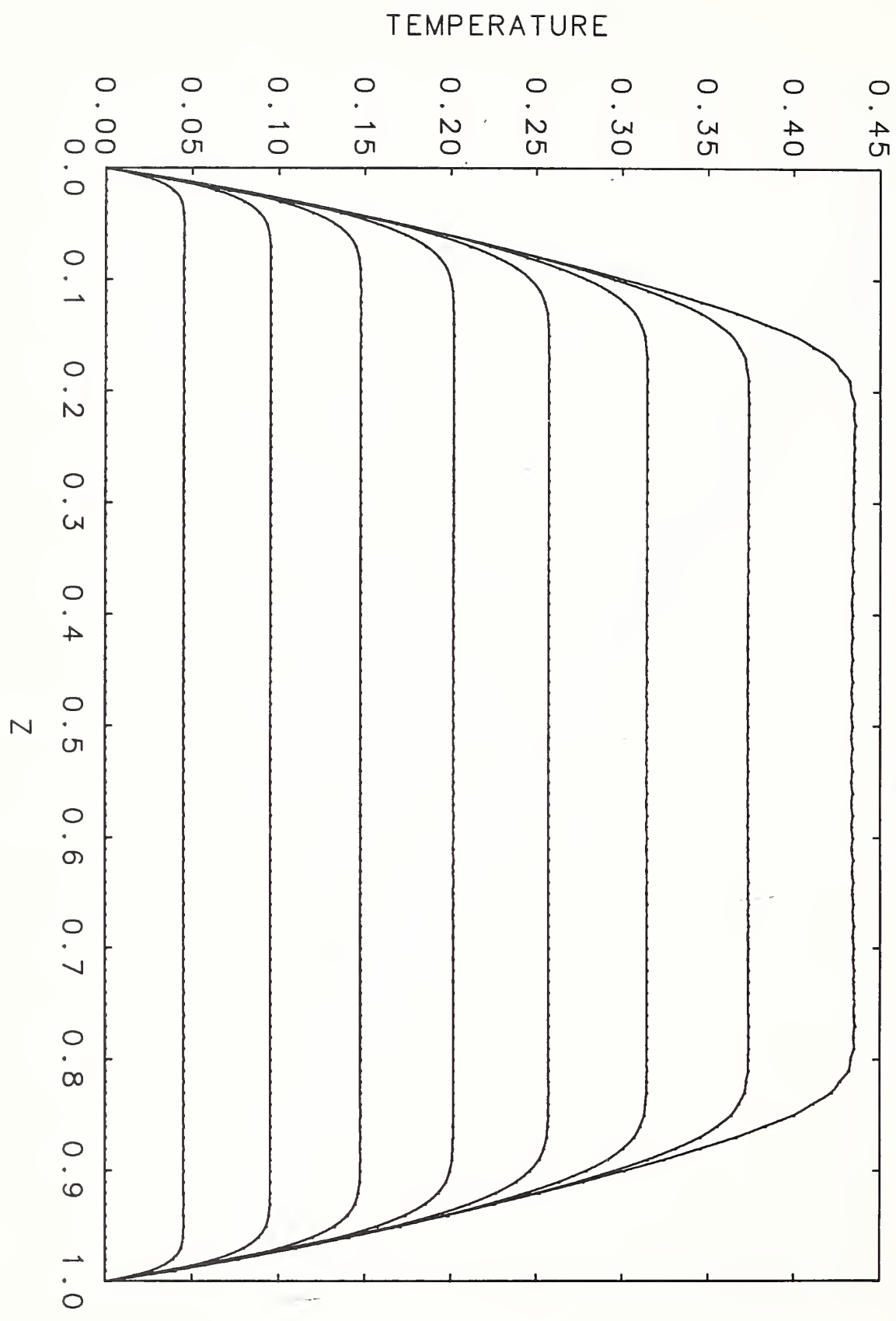


FIG. 1(d)

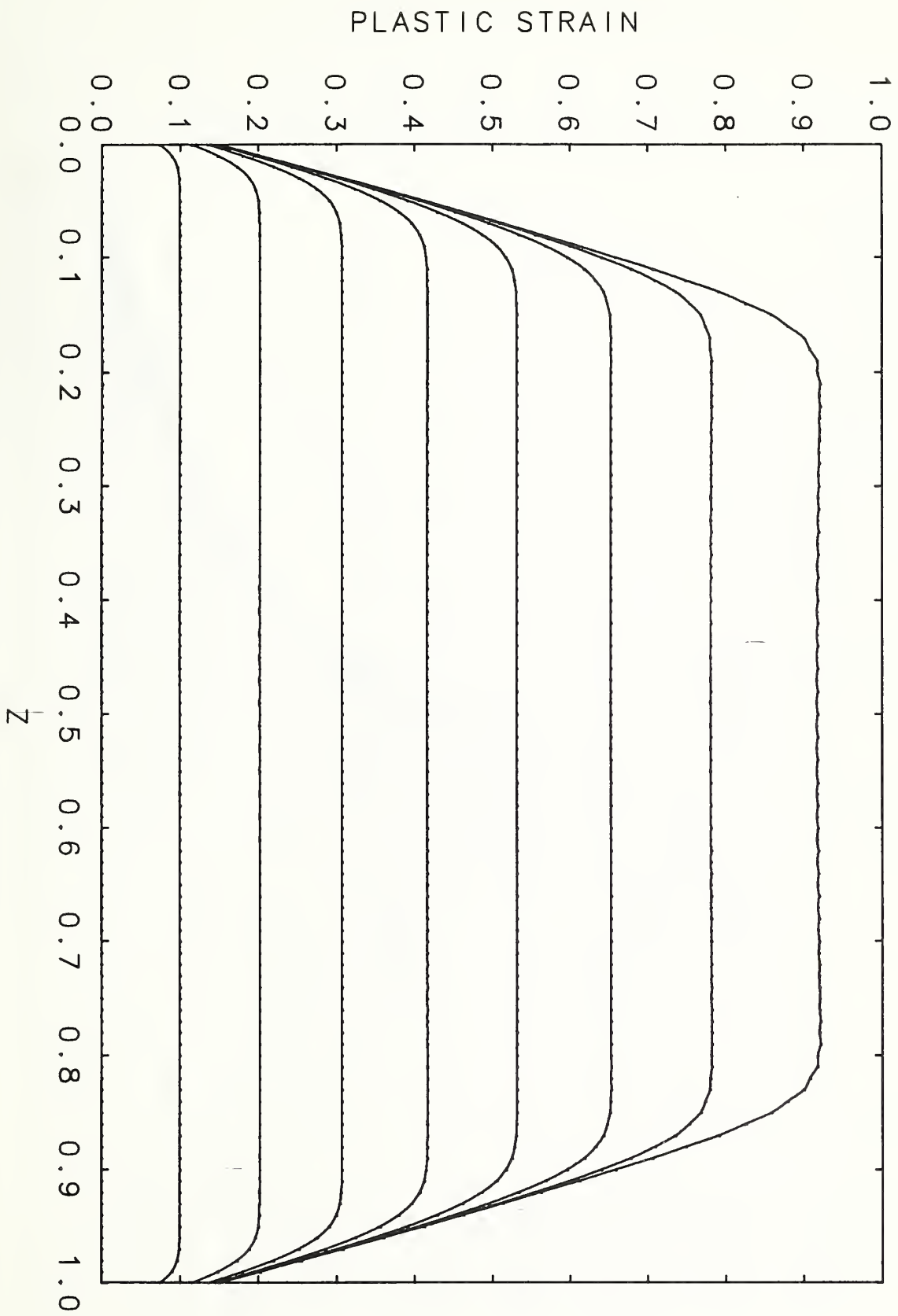
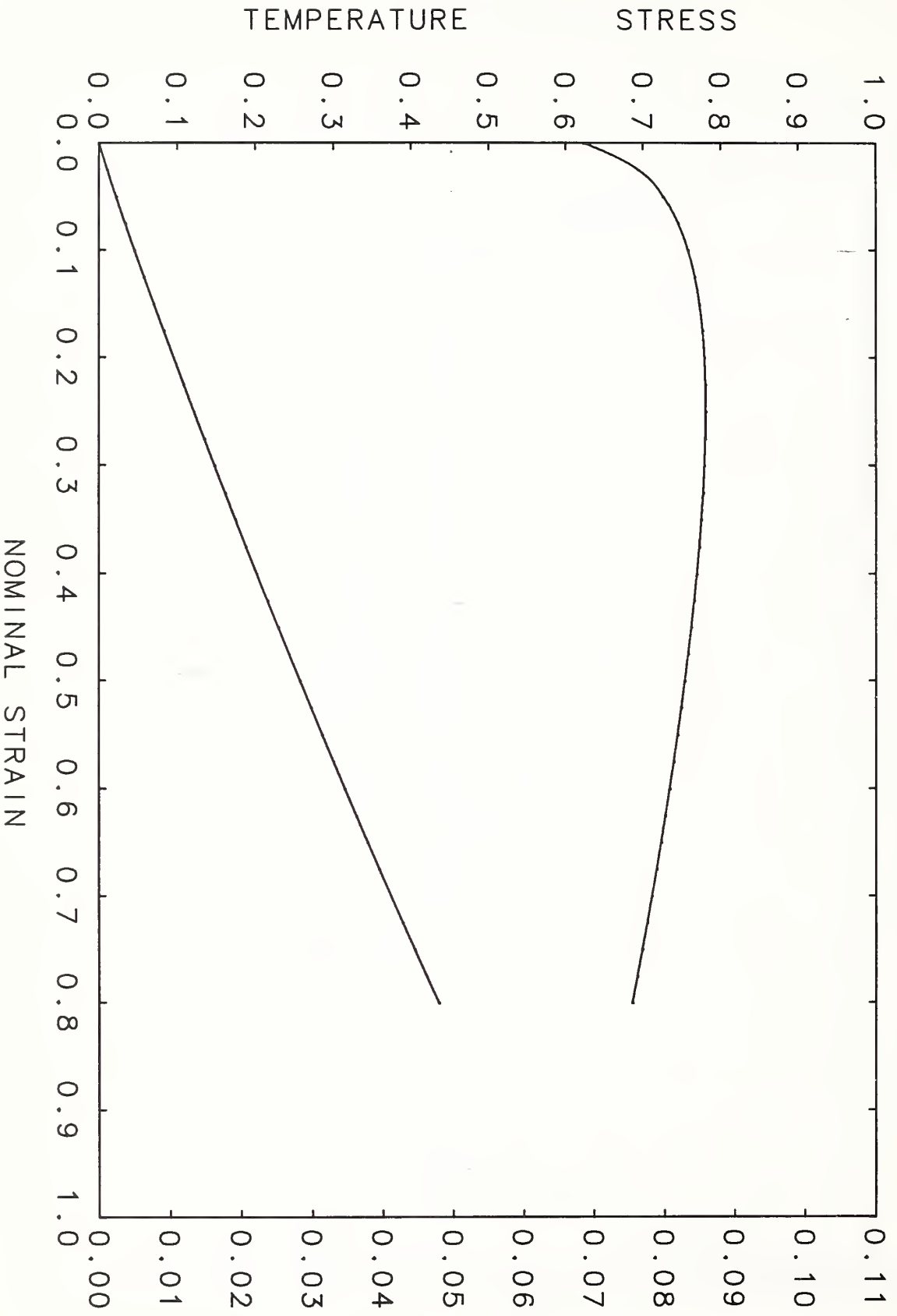


FIG. 2



TWIST

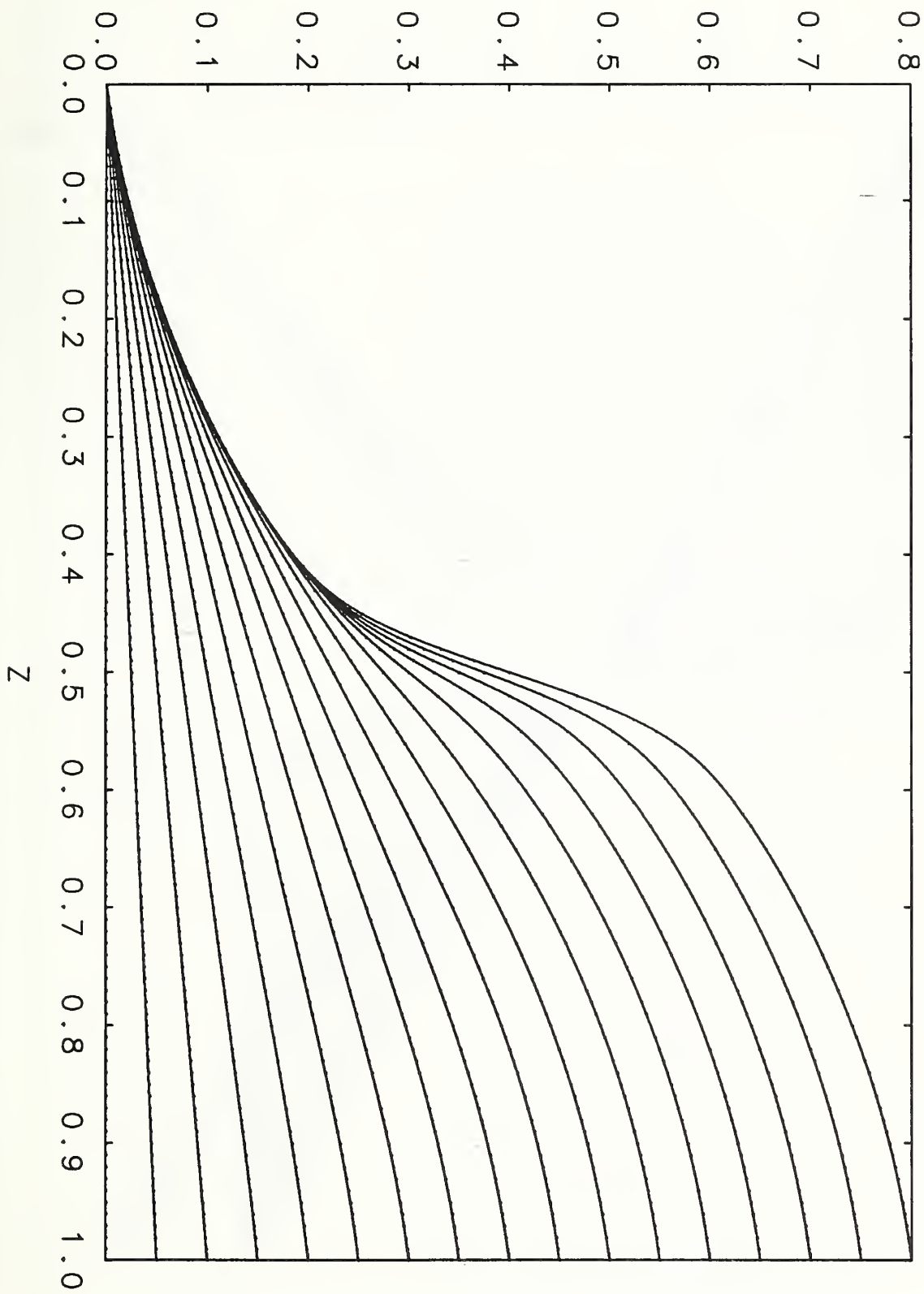
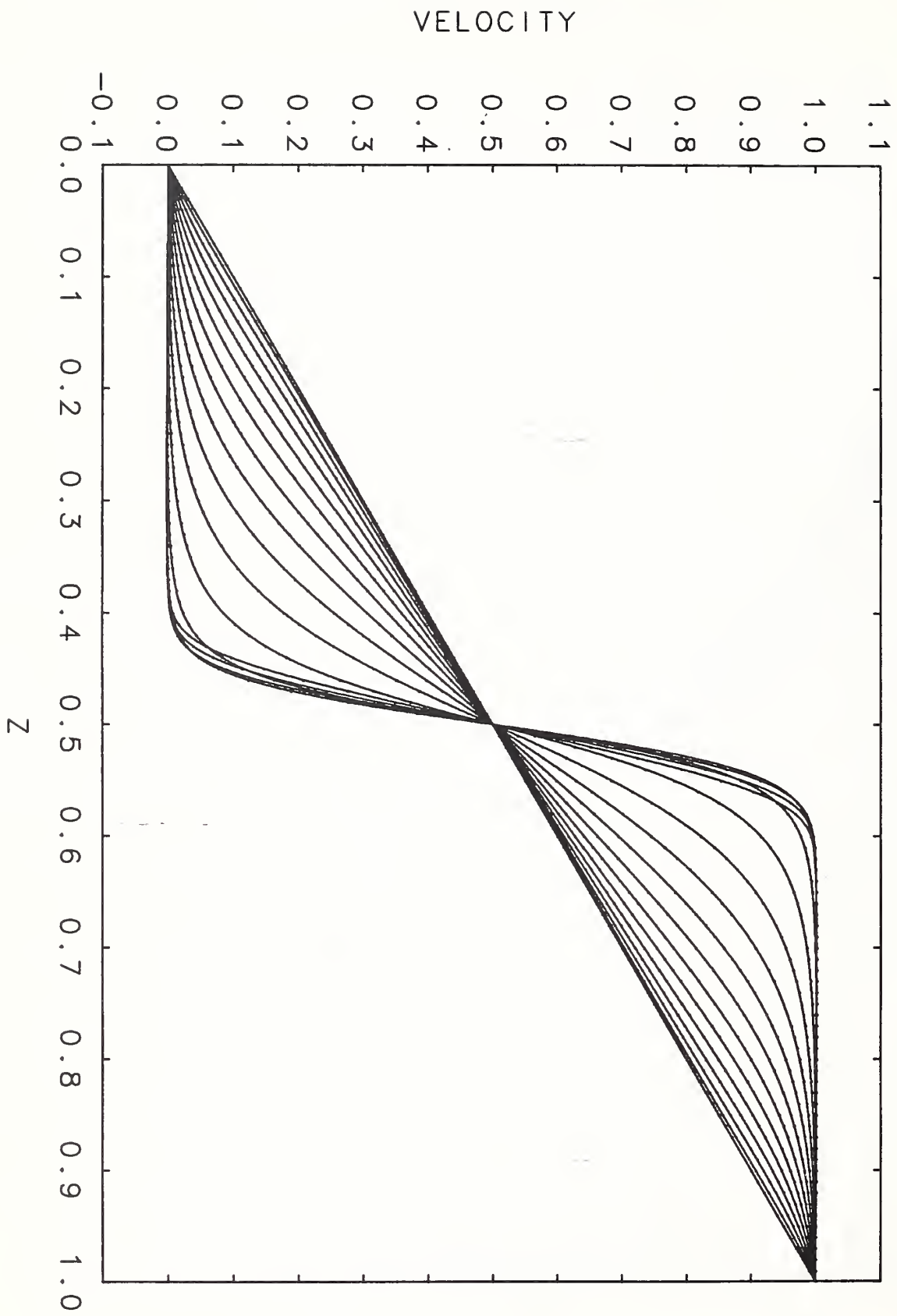


FIG. 3(a)

FIG. 3(b)



TEMPERATURE

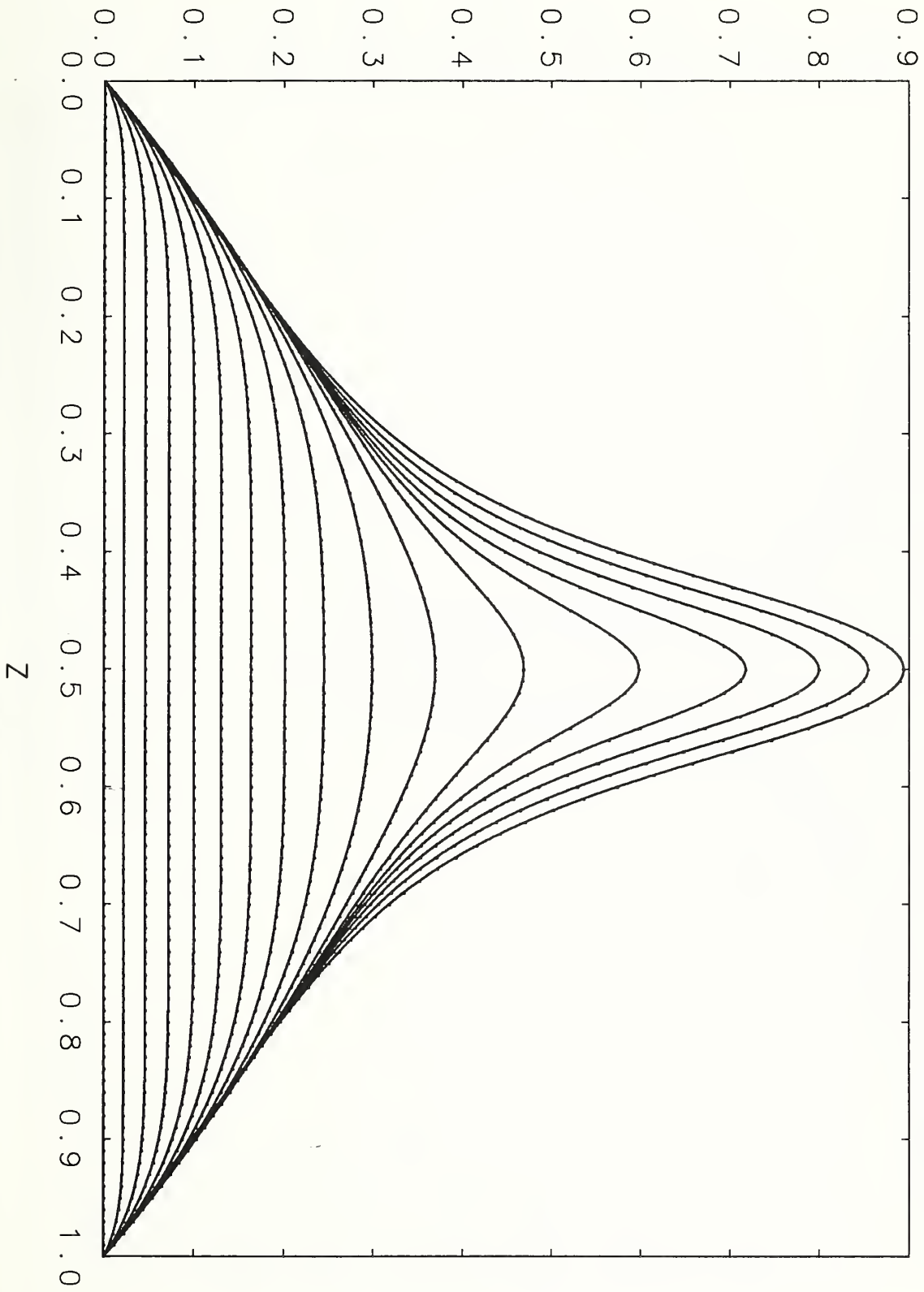
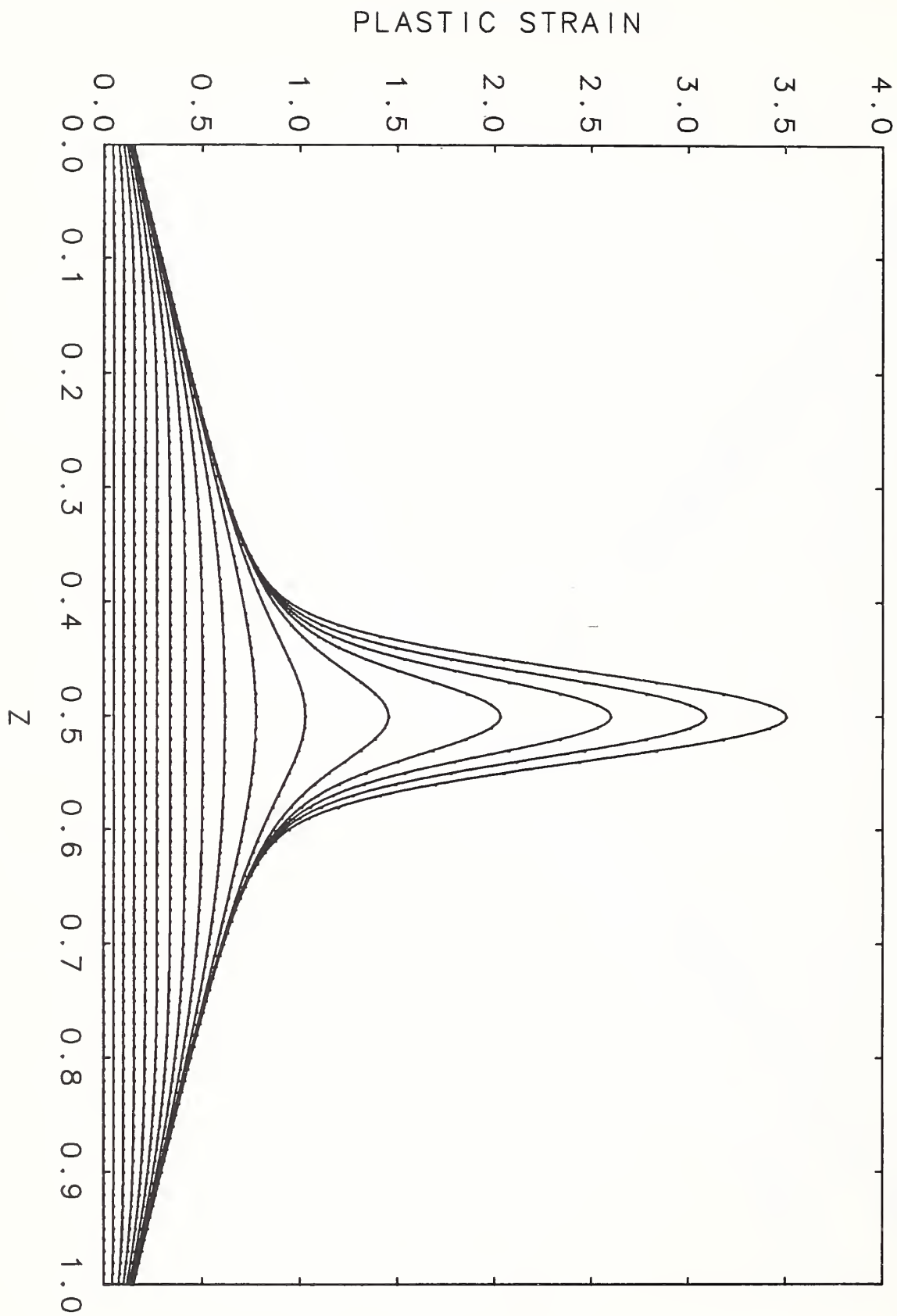


FIG. 3(c)

FIG. 3(d)



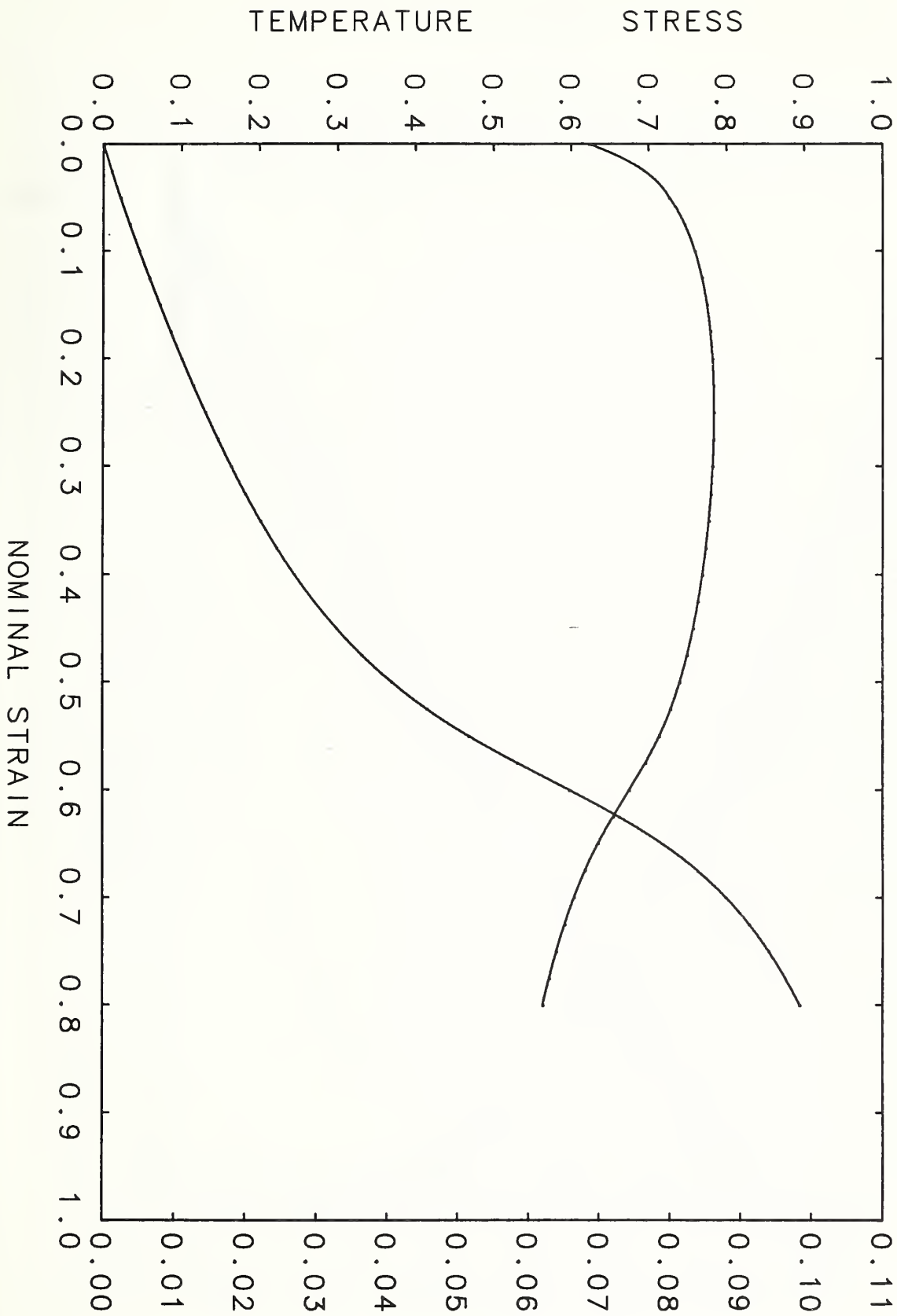


FIG. 4

FIG. 5(a)

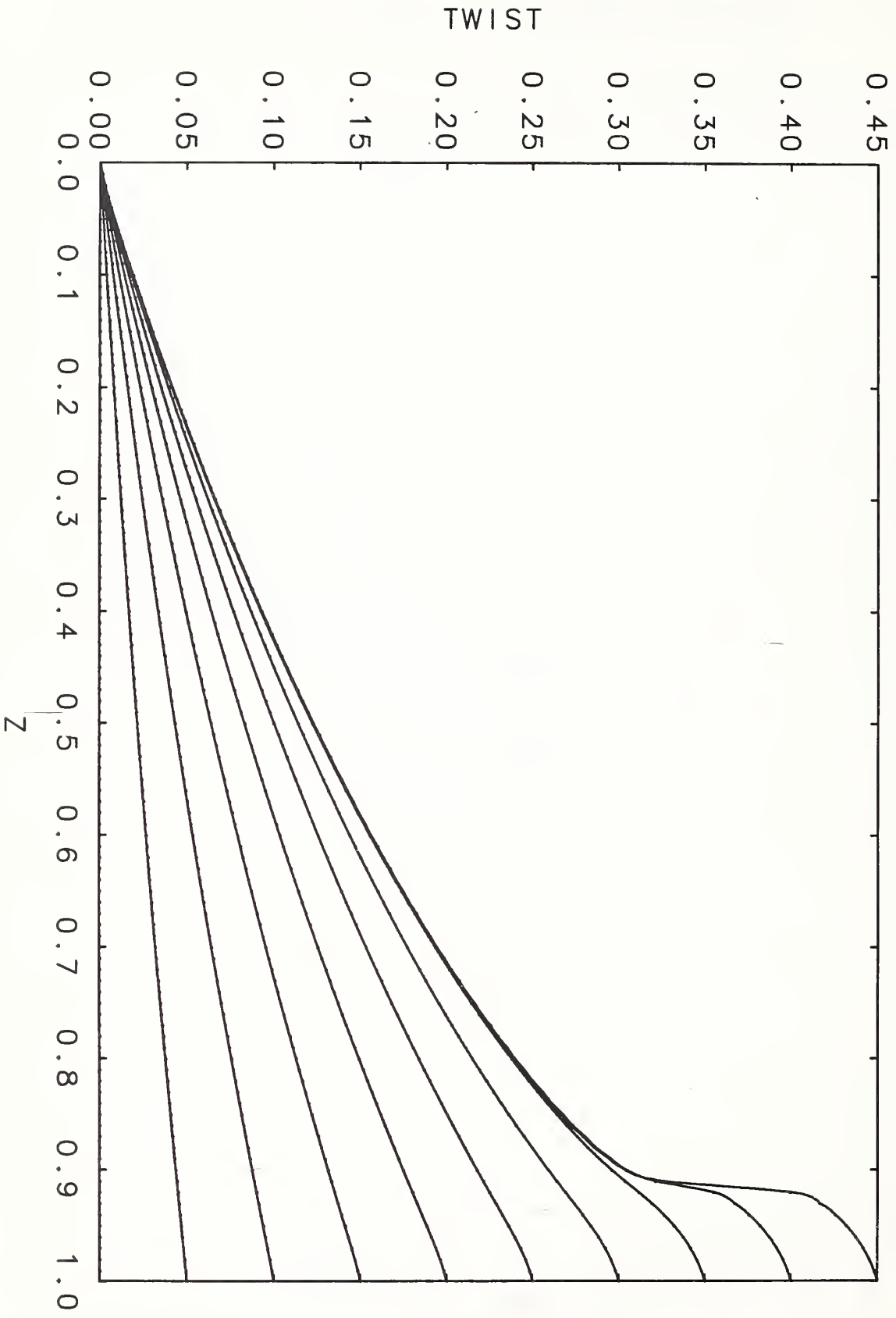


FIG. 5(b)

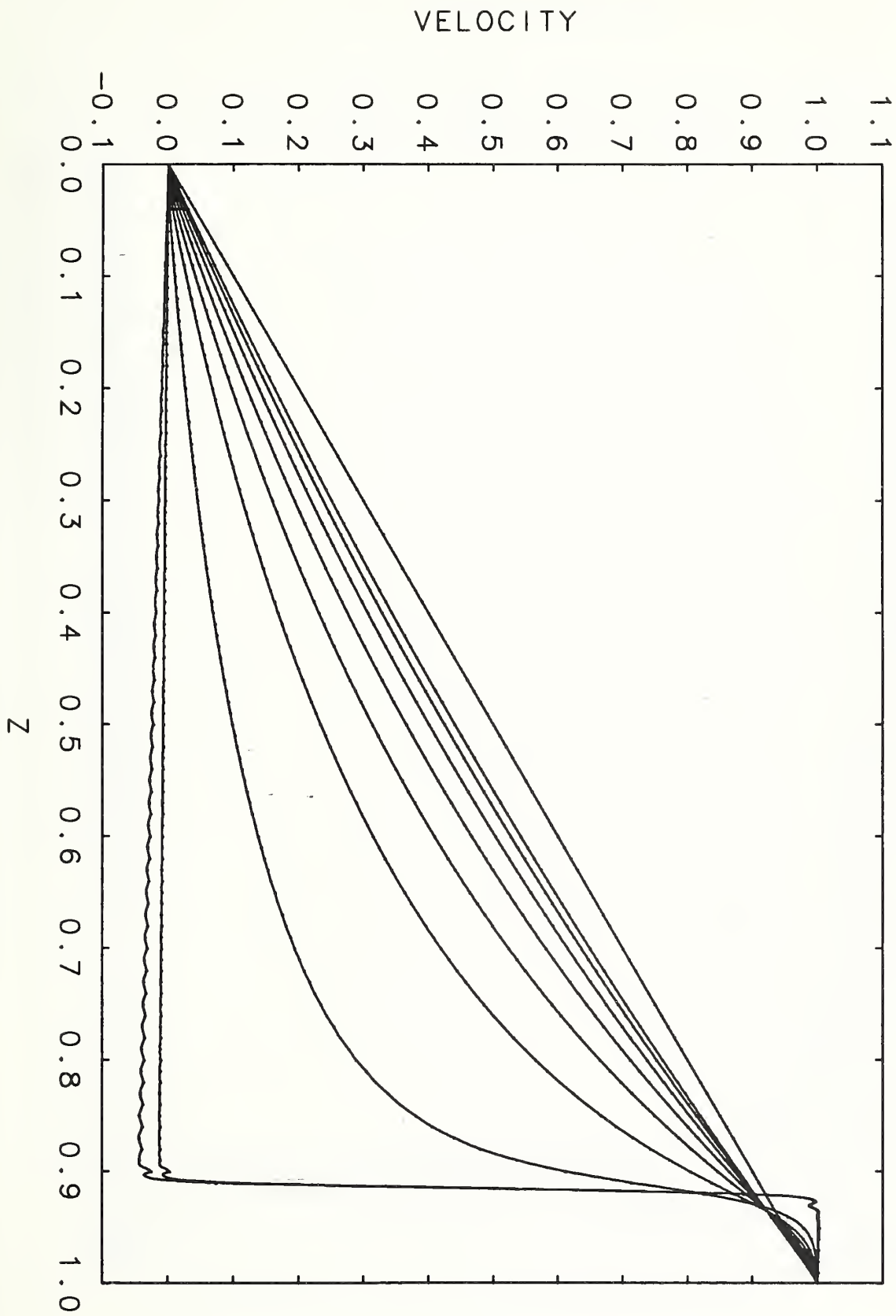
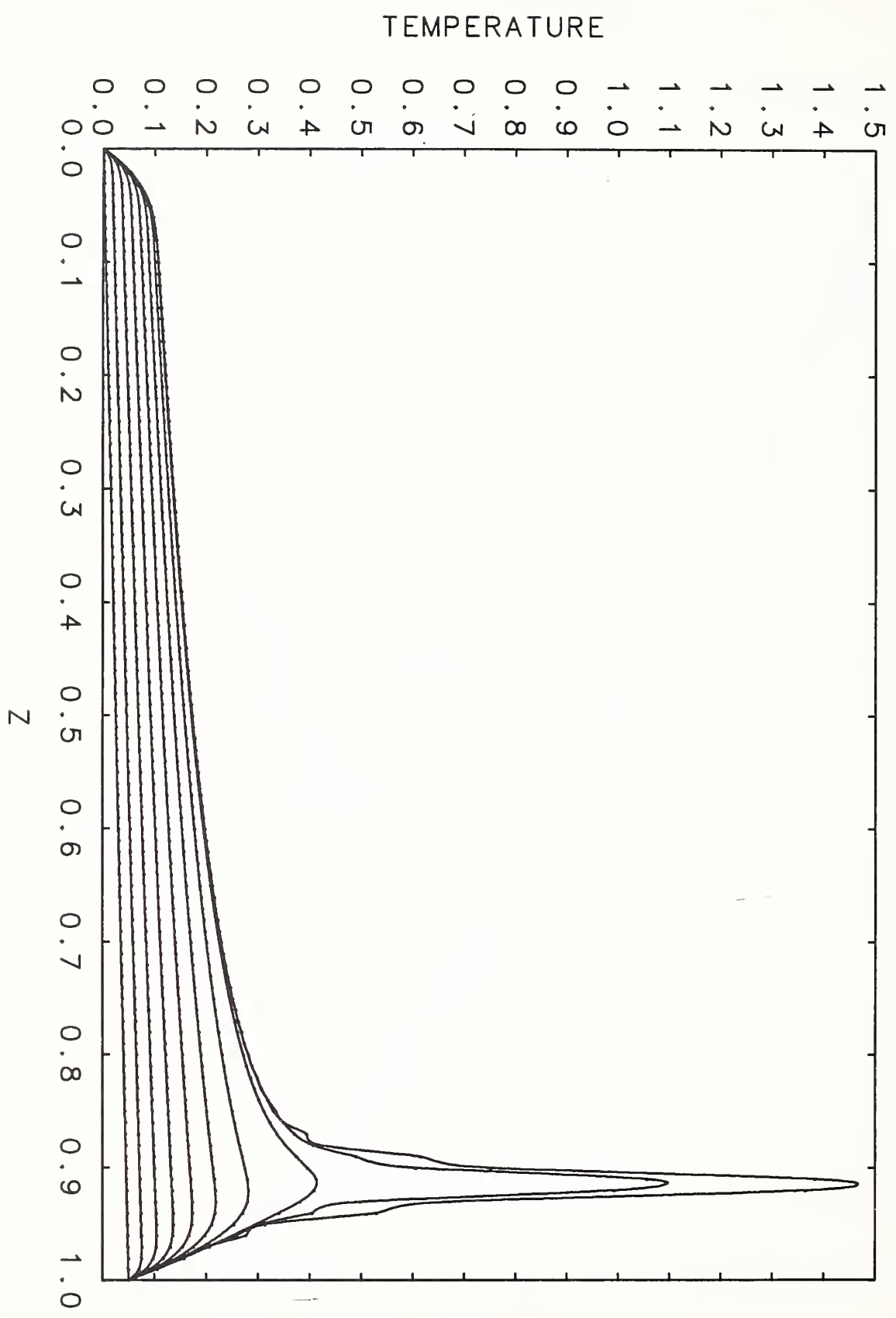


FIG. 5(c)



PLASTIC STRAIN

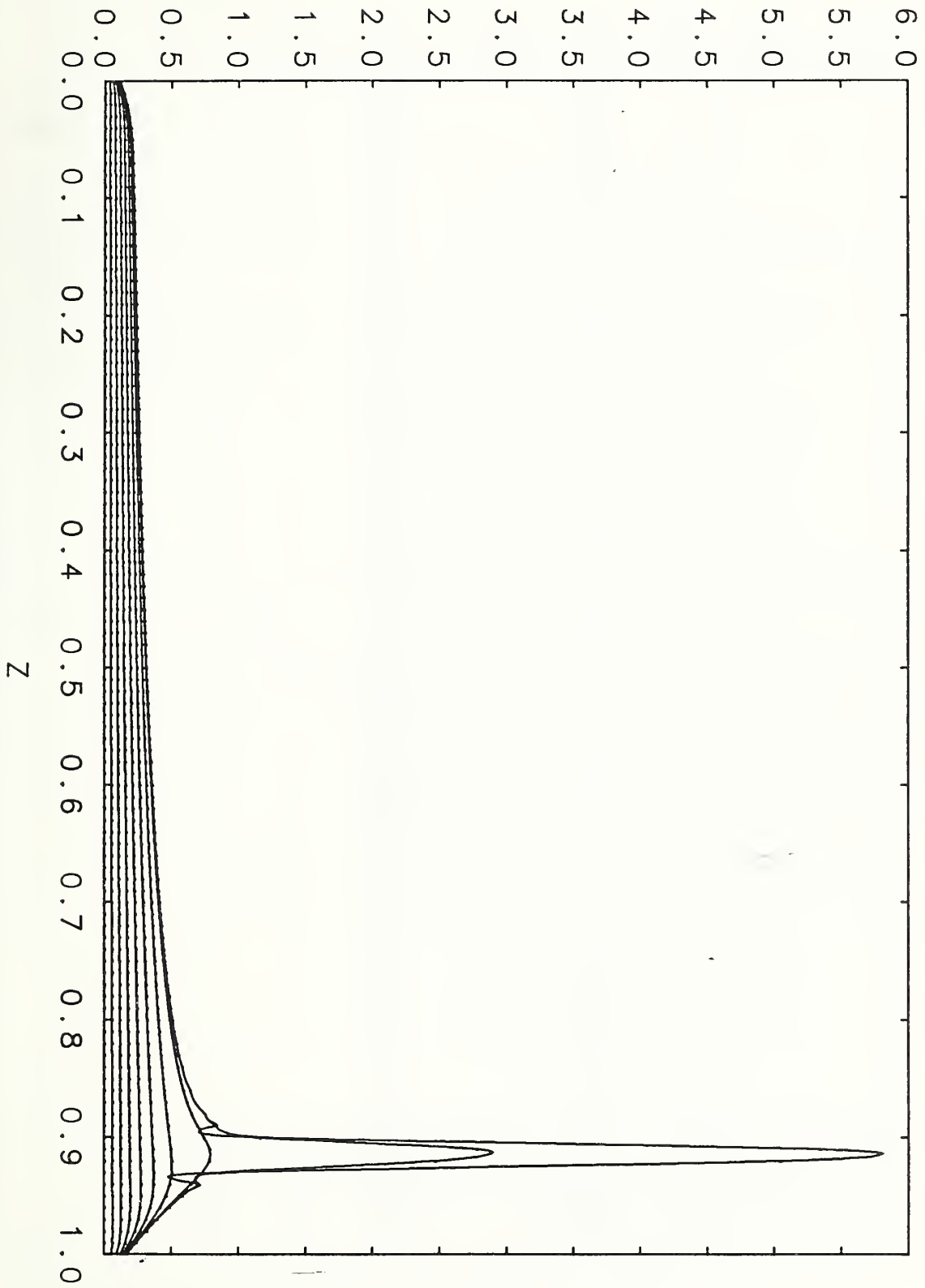
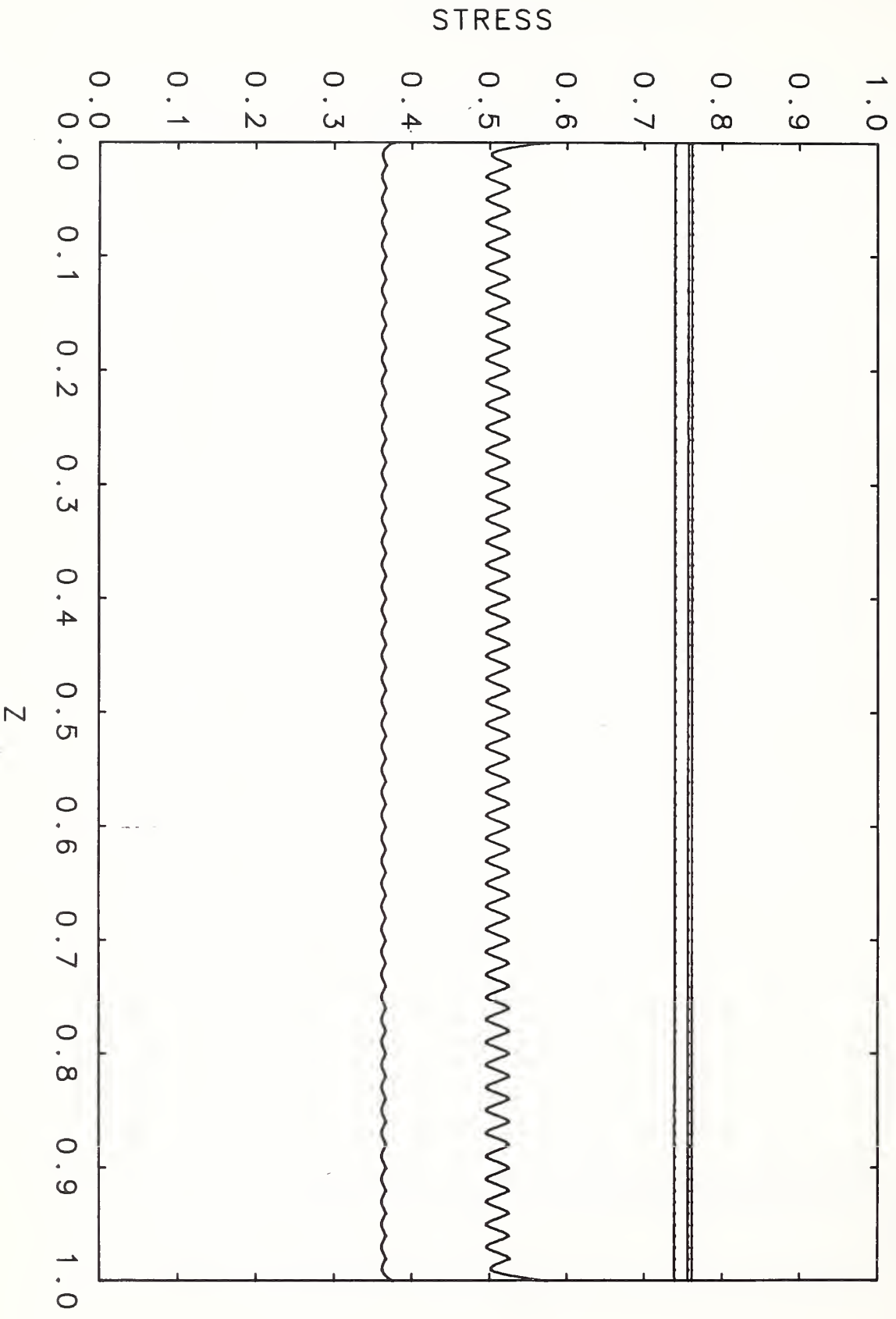


FIG. 5(d)

FIG. 5(e)



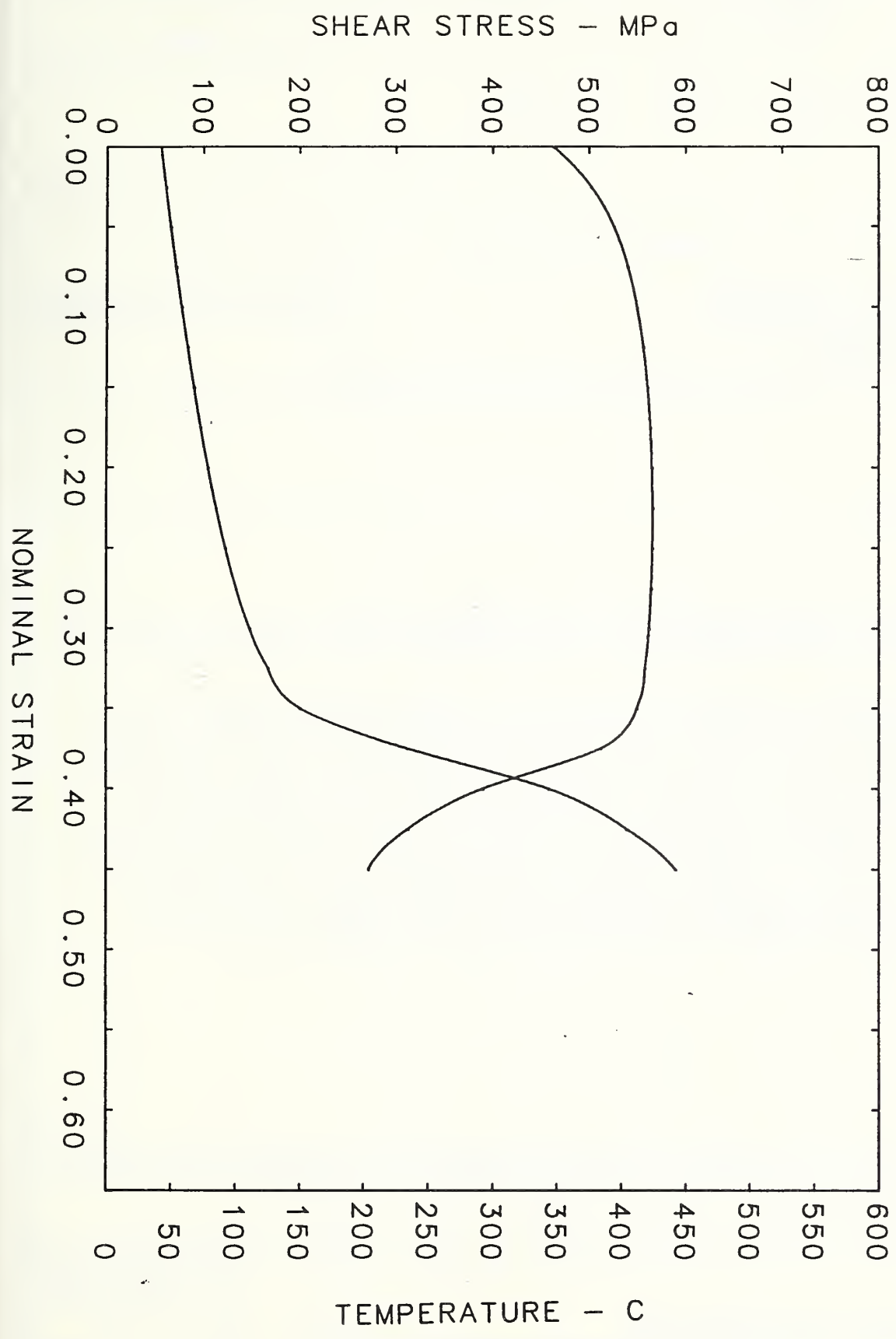


FIG. 6

U.S. DEPT. OF COMM. BIBLIOGRAPHIC DATA SHEET (See instructions)	1. PUBLICATION OR REPORT NO. NISTIR 89-4121	2. Performing Organ. Report No.	3. Publication Date July 1989
4. TITLE AND SUBTITLE A Mechanism for Shear Band Formation in the High Strain Rate Torsion Test			
5. AUTHOR(S) Timothy J. Burns			
6. PERFORMING ORGANIZATION (If joint or other than NBS, see instructions) NATIONAL BUREAU OF STANDARDS U.S. DEPARTMENT OF COMMERCE GAITHERSBURG, MD 20899		7. Contract/Grant No.	8. Type of Report & Period Covered
9. SPONSORING ORGANIZATION NAME AND COMPLETE ADDRESS (Street, City, State, ZIP)			
10. SUPPLEMENTARY NOTES <input type="checkbox"/> Document describes a computer program; SF-185, FIPS Software Summary, is attached.			
11. ABSTRACT (A 200-word or less factual summary of most significant information. If document includes a significant bibliography or literature survey, mention it here) An asymptotics argument is given, which shows that rigid unloading from the ends of the thin-walled tubular specimen, enhanced by conductive heat transfer, is a plausible mechanism for adiabatic shear band formation during the high strain rate torsion test. The argument assumes that thickness variations, as well as elastic and dynamic effects in the tube, can be ignored, but that heat conduction and heat-sink thermal boundary conditions must be included. The proposed mechanism is supported by a numerical analysis of a mathematical model of the torsion test, which is based on recent torsional Kolsky bar experimental work of Marchand and Duffy (1988), on a physical model of thermoelastic-plastic flow due to Wallace (1985), and on a phenomenological Arrhenius model of the plastic flow surface. The numerical technique used is the semi-discretization method of lines.			
12. KEY WORDS (Six to twelve entries; alphabetical order; capitalize only proper names; and separate key words by semicolons) adiabatic shear; torsion test; material instability, viscoplasticity			
13. AVAILABILITY <input checked="" type="checkbox"/> Unlimited <input type="checkbox"/> For Official Distribution. Do Not Release to NTIS <input type="checkbox"/> Order From Superintendent of Documents, U.S. Government Printing Office, Washington, D.C. 20402. <input checked="" type="checkbox"/> Order From National Technical Information Service (NTIS), Springfield, VA. 22161		14. NO. OF PRINTED PAGES 45	15. Price \$12.95

